Dust-Radiation Interaction

Funded by the European Union

GA No 101160258

Vincenzo Obiso and Carlos Pérez García-Pando
BSC and ICREA

Outline of the session

- An introduction to dust effects and feedbacks
- Dust radiative effect and forcing
- The impontance of size, shape and mineralogical composition (EMIT)
- Constraining the global dust SSA with constrained PSDs and mineralogy
- Dust radiation impacts on weather forecasting

Dust effects and feedbacks

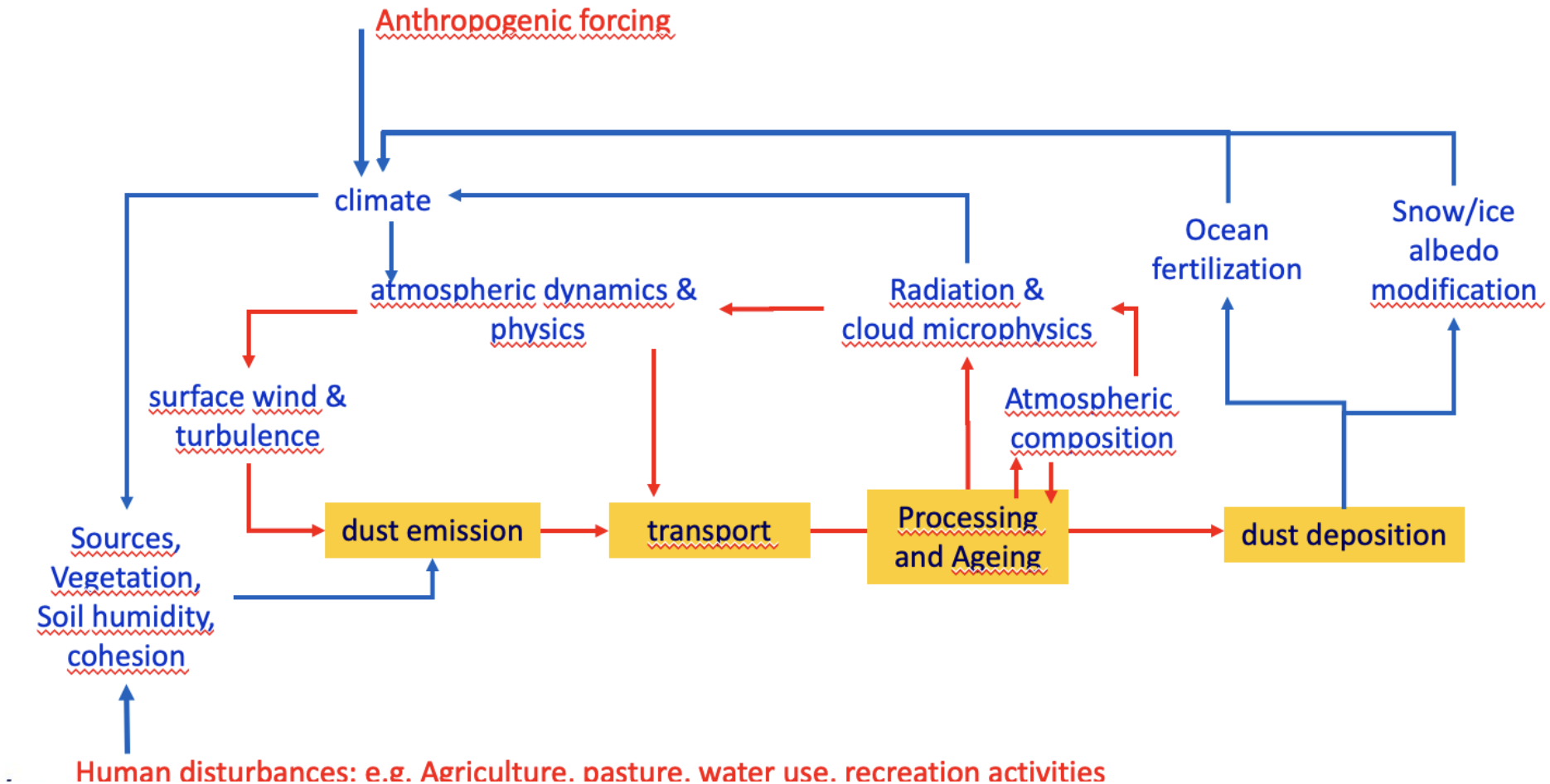

Global radiative effect and forcing

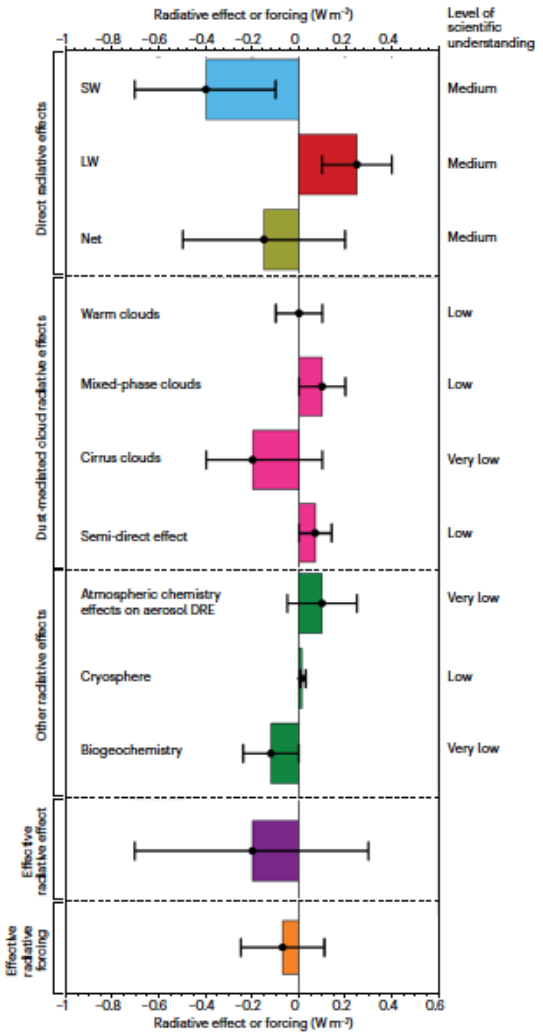

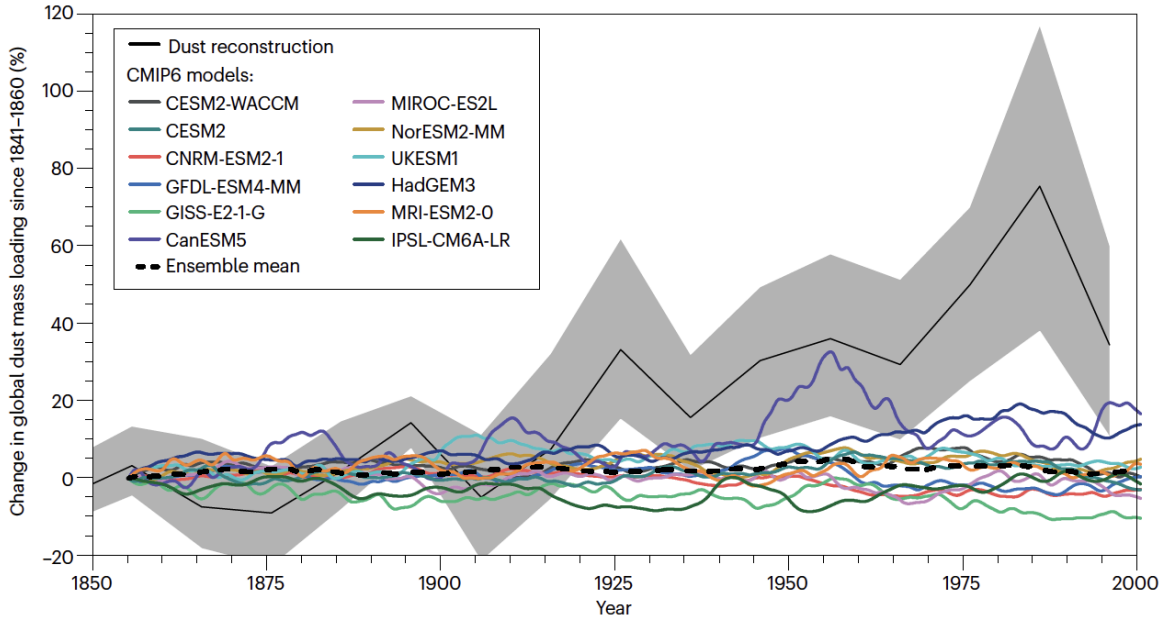

Dust interactions with radiation (direct effects)

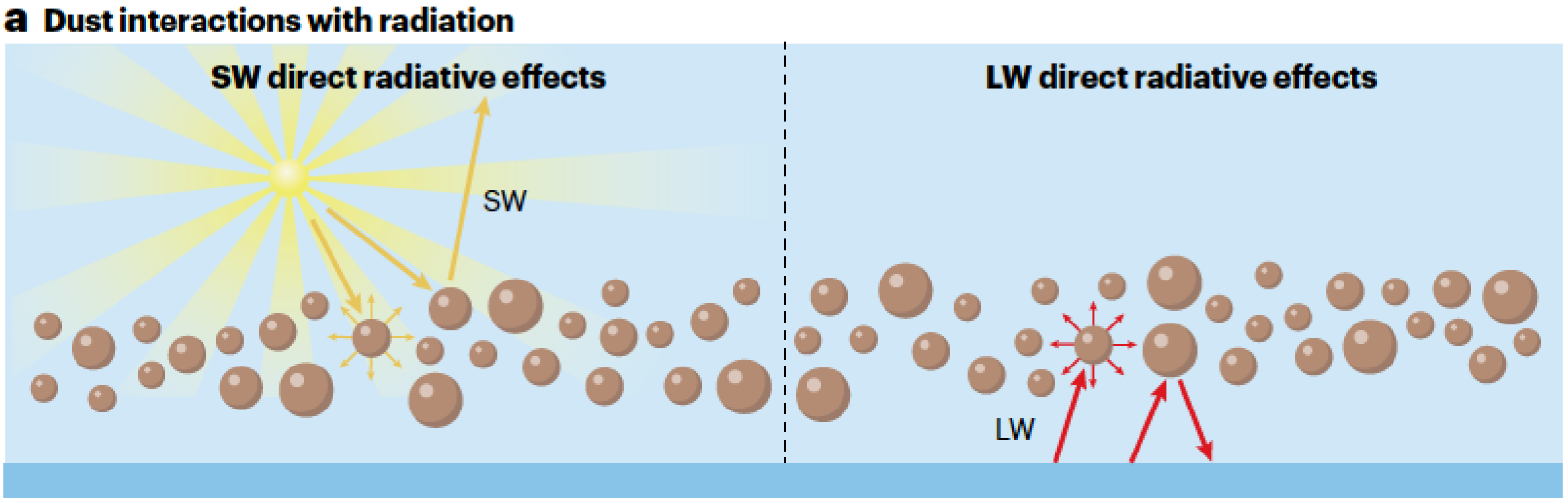

Modeling the direct radiative effect

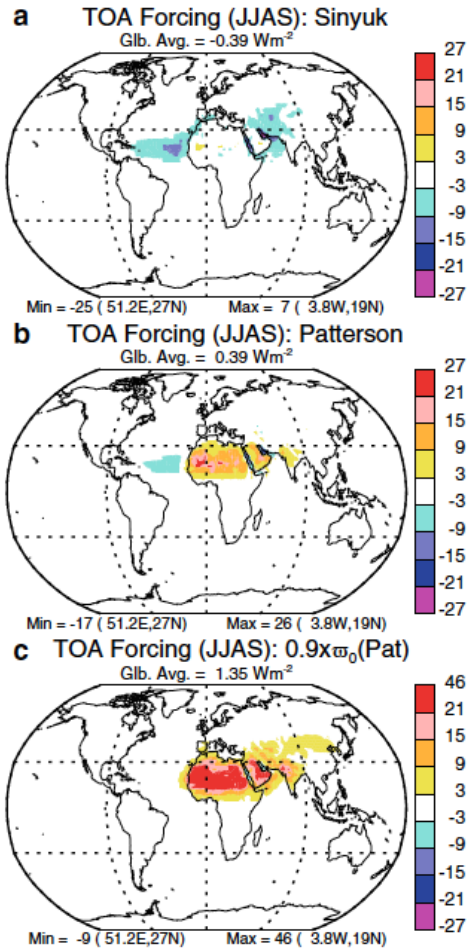

More scattering dust

More absorbing dust

Miller et al. (2014)

DRE uncertainty due to soil mineralogy

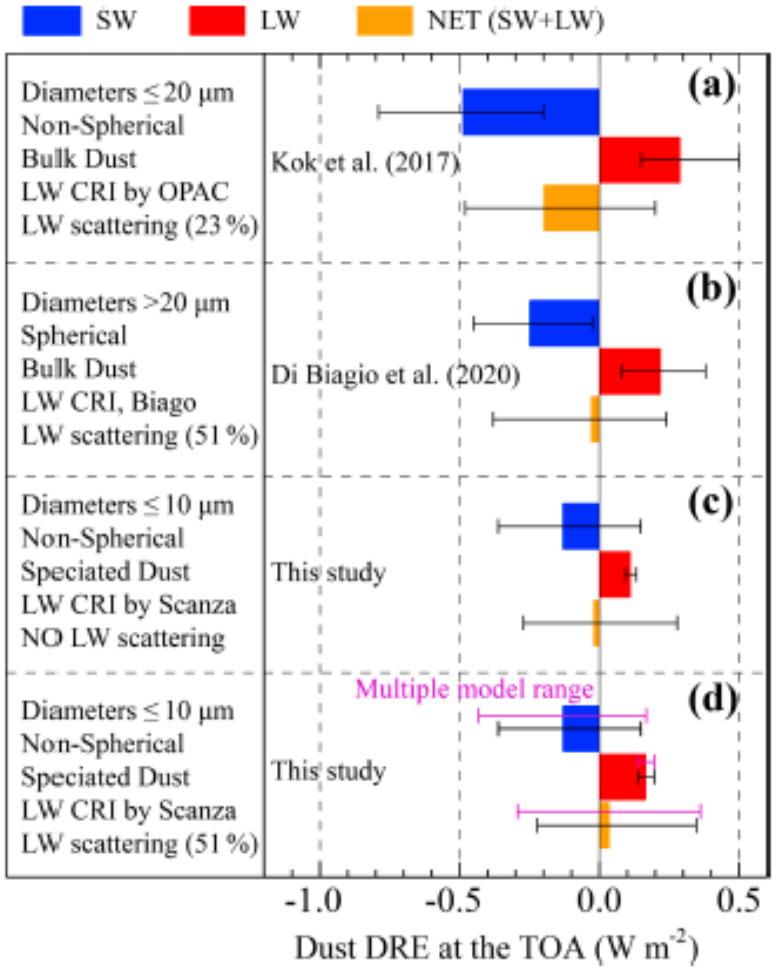

Today, when using mineral speciation in models:

- The global net TOA DRE is estimated to be -0.23 to +0.35 m^2 due to soil mineralogy uncertainty

- 97 % of this range is related to the abundance of iron oxides

Li et al. (2021)

The importance of meteorological composition

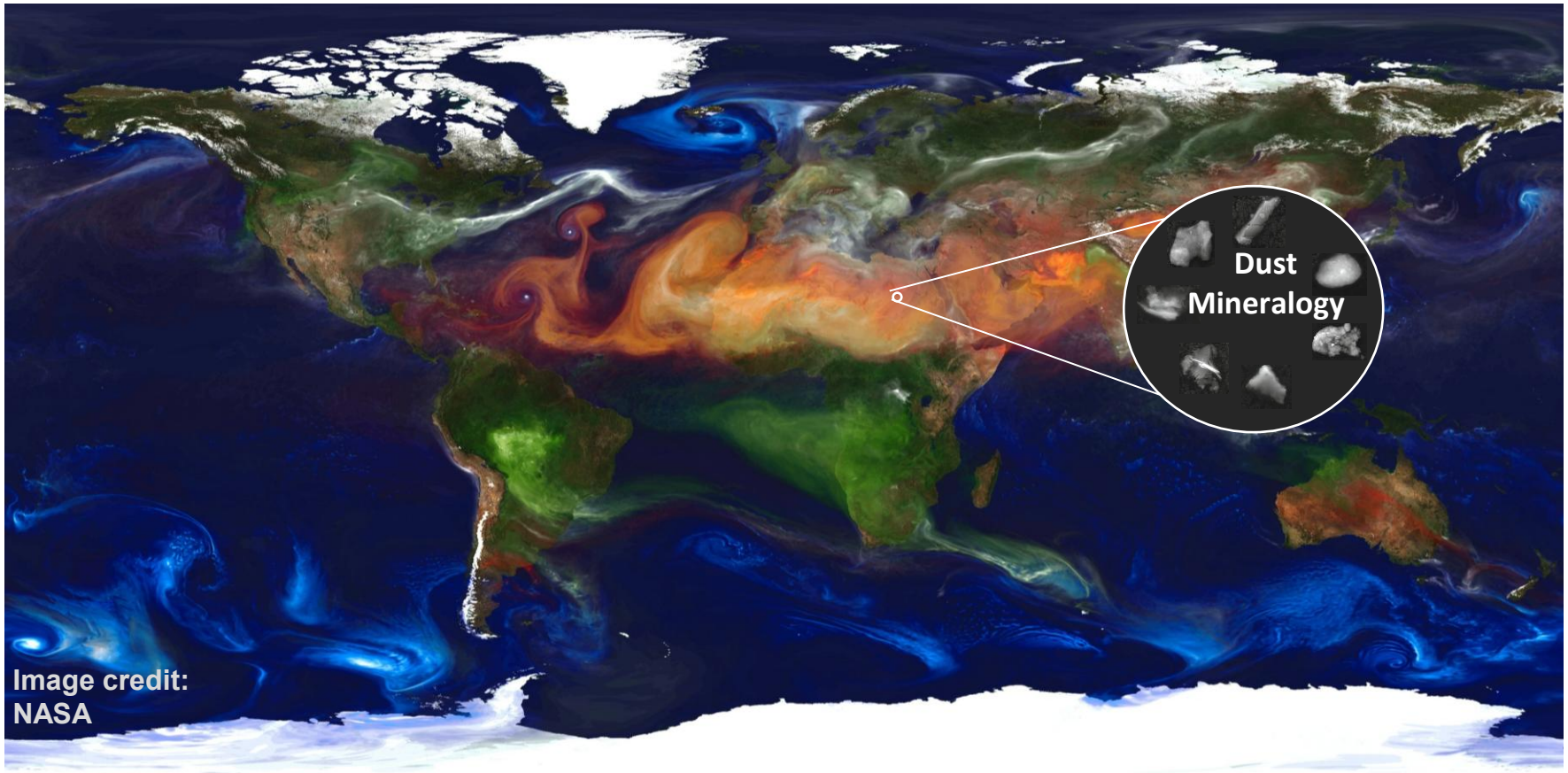

The importance of meteorological composition

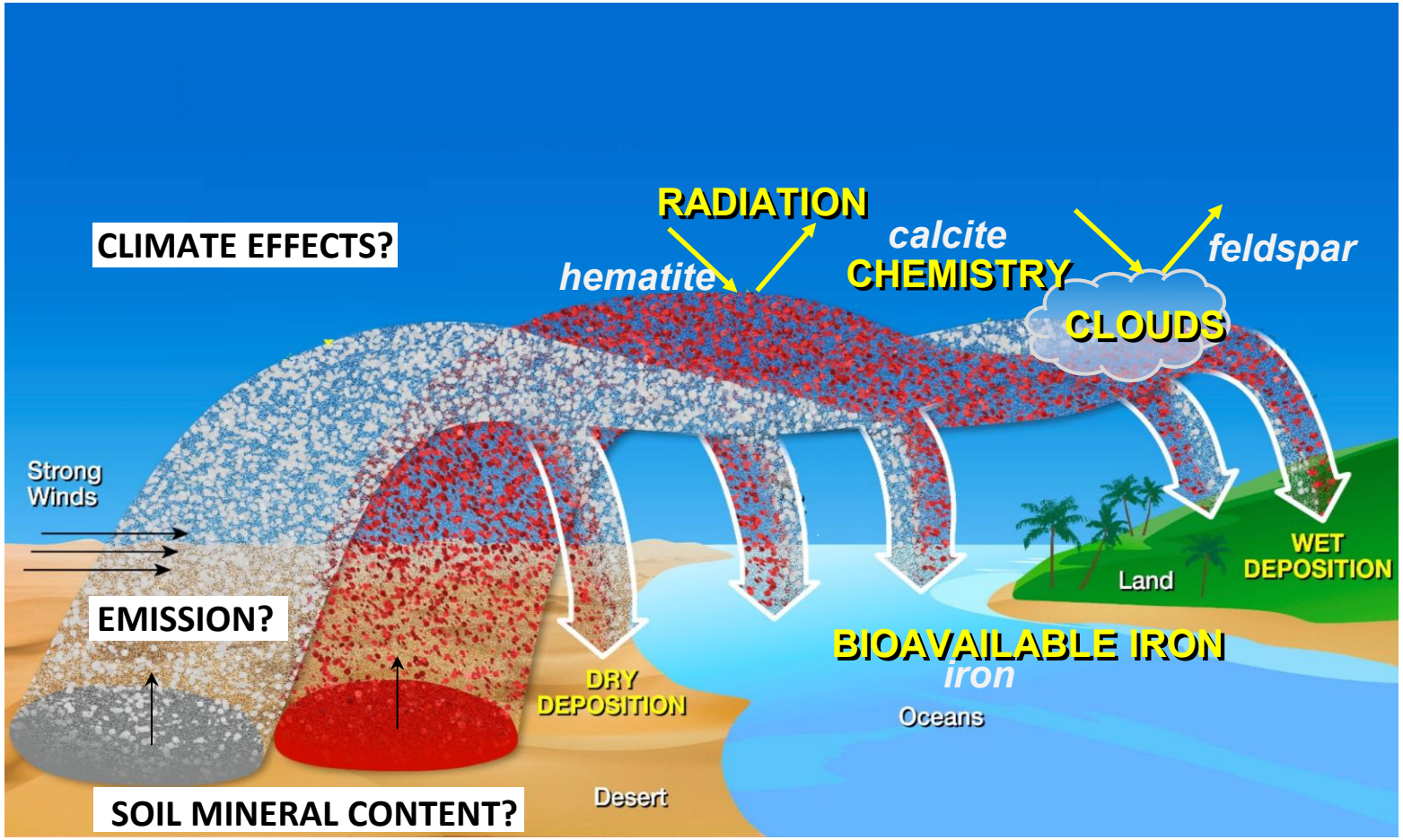

Models neglect dust mineralogical composition variations

- Traditionally: Model an ‘average’ mineral aerosol
- Mineral aerosols are from different minerals depending on surface composition

Each mineral has different properties and interactions with Earth System

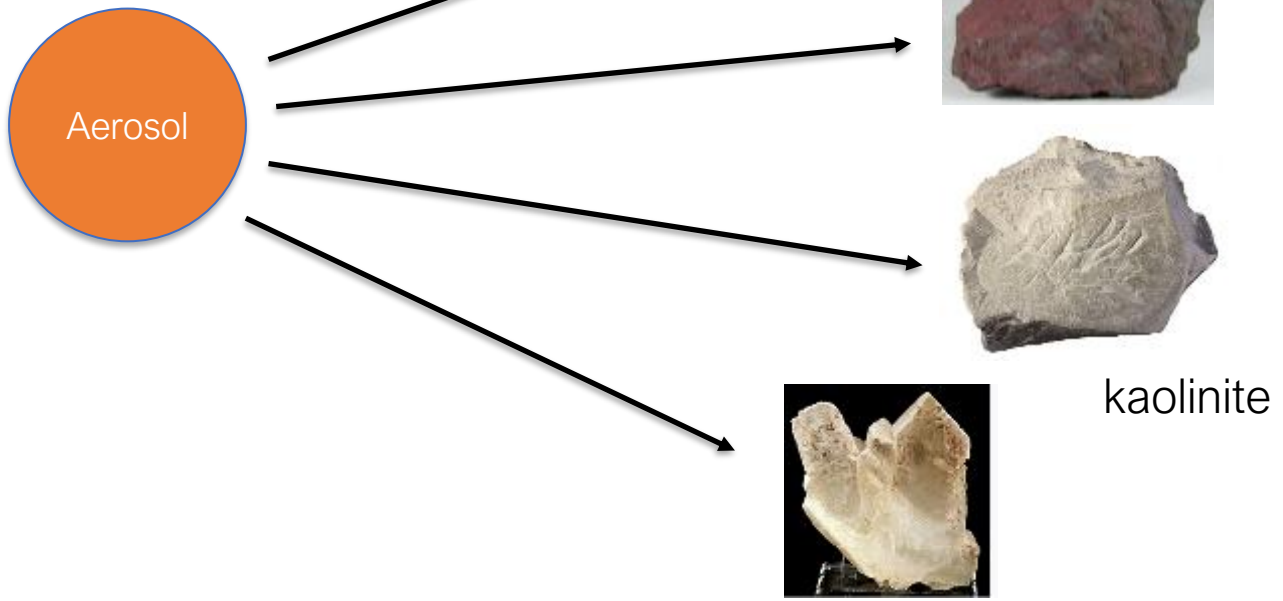

Illite

hematite

Iron oxides:
Absorb short wavelength (SW), iron for ocean biogeochemistry, low pH

Kaolinite:
Reflects SW, high pH

kaolinite

Clays, large particles:
Reflects SW

montmorillonite

Shortwave radiative effects

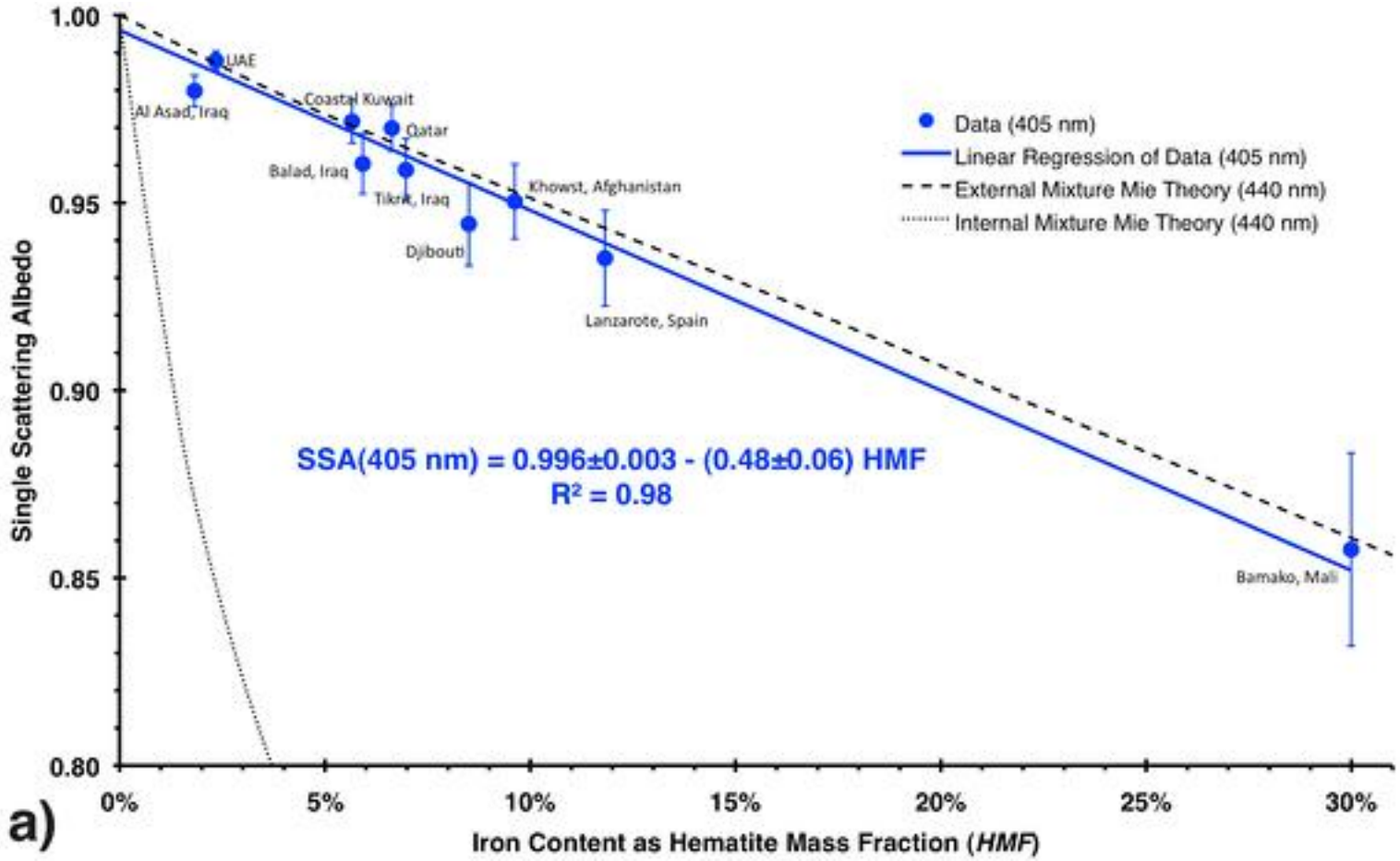

Moosmüller et al. (2012)

Iron oxides
Hematite

Longwave radiative effects

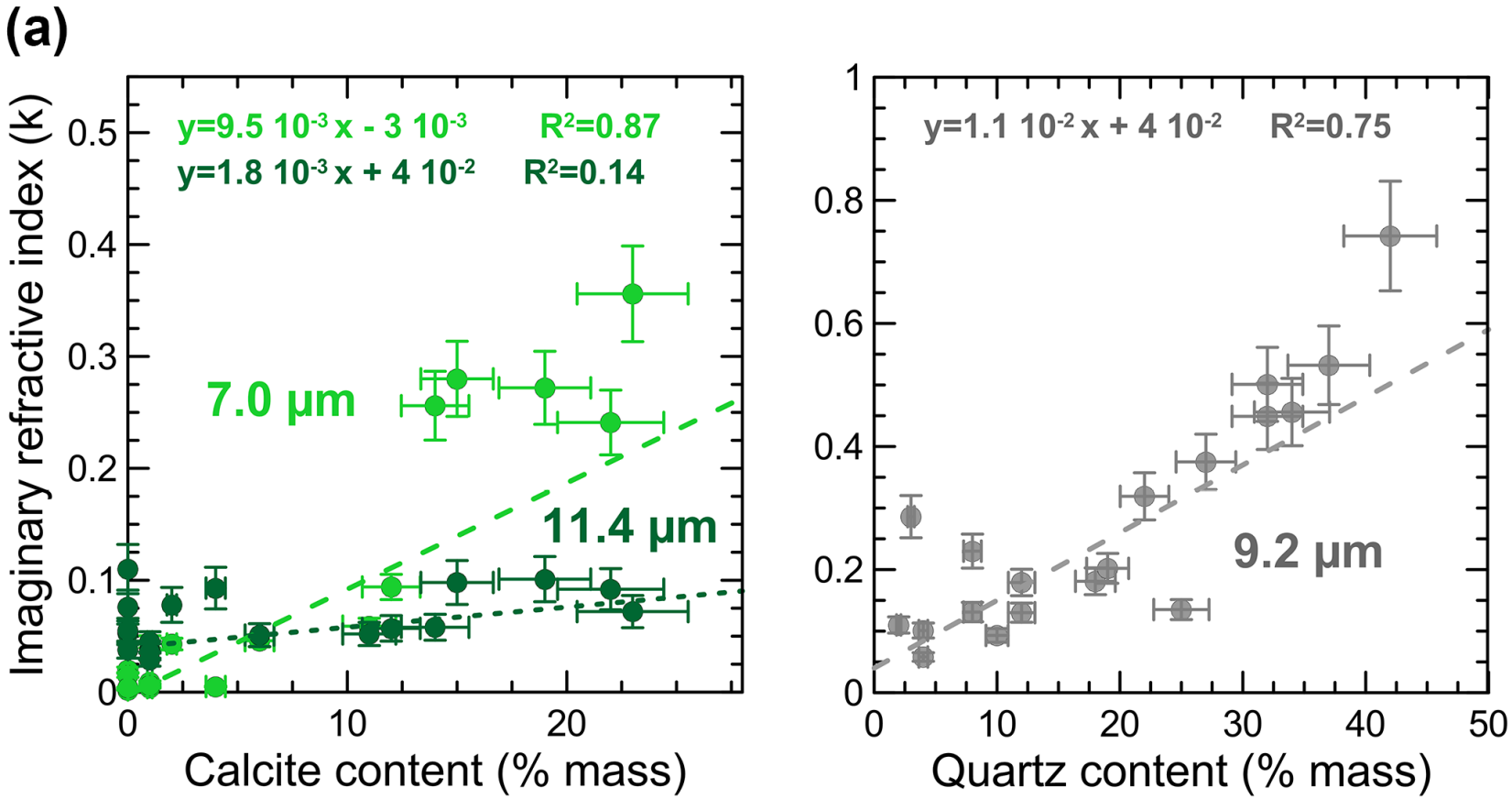

Di Biagio et al. (2017)

Calcite
Quartz

Mapping of soil-surface mineralogy

Claquin et al., 1999; Journet et al., 2014

- Currently 12 key minerals estimated
- 700 soil descriptions sampling 55 % of FAO soil units
- Many regions including prolific sources not sampled
- Massive extrapolation based on soil unit/type
- A number of assumptions to overcome the lack of data: for example on hematite and goethite size

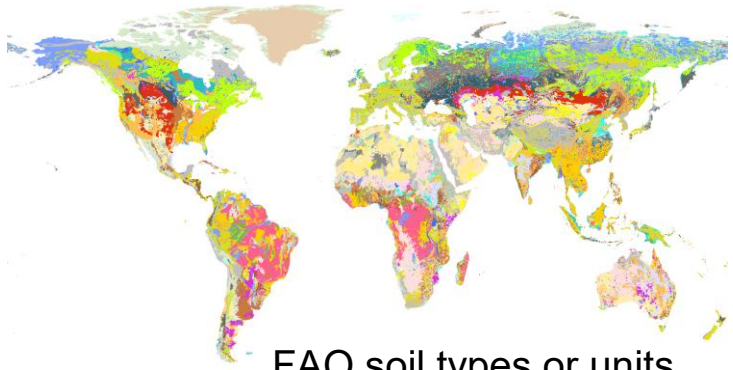

FAO soil types or units

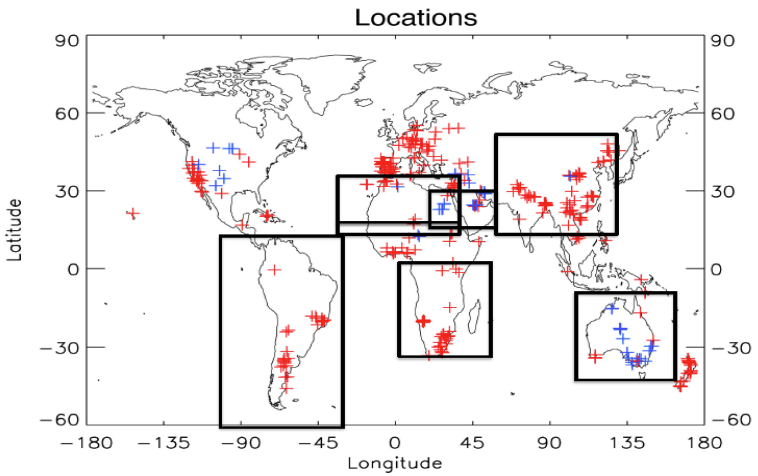

The Earth surface Mineral dust source InvesTigation (EMIT)

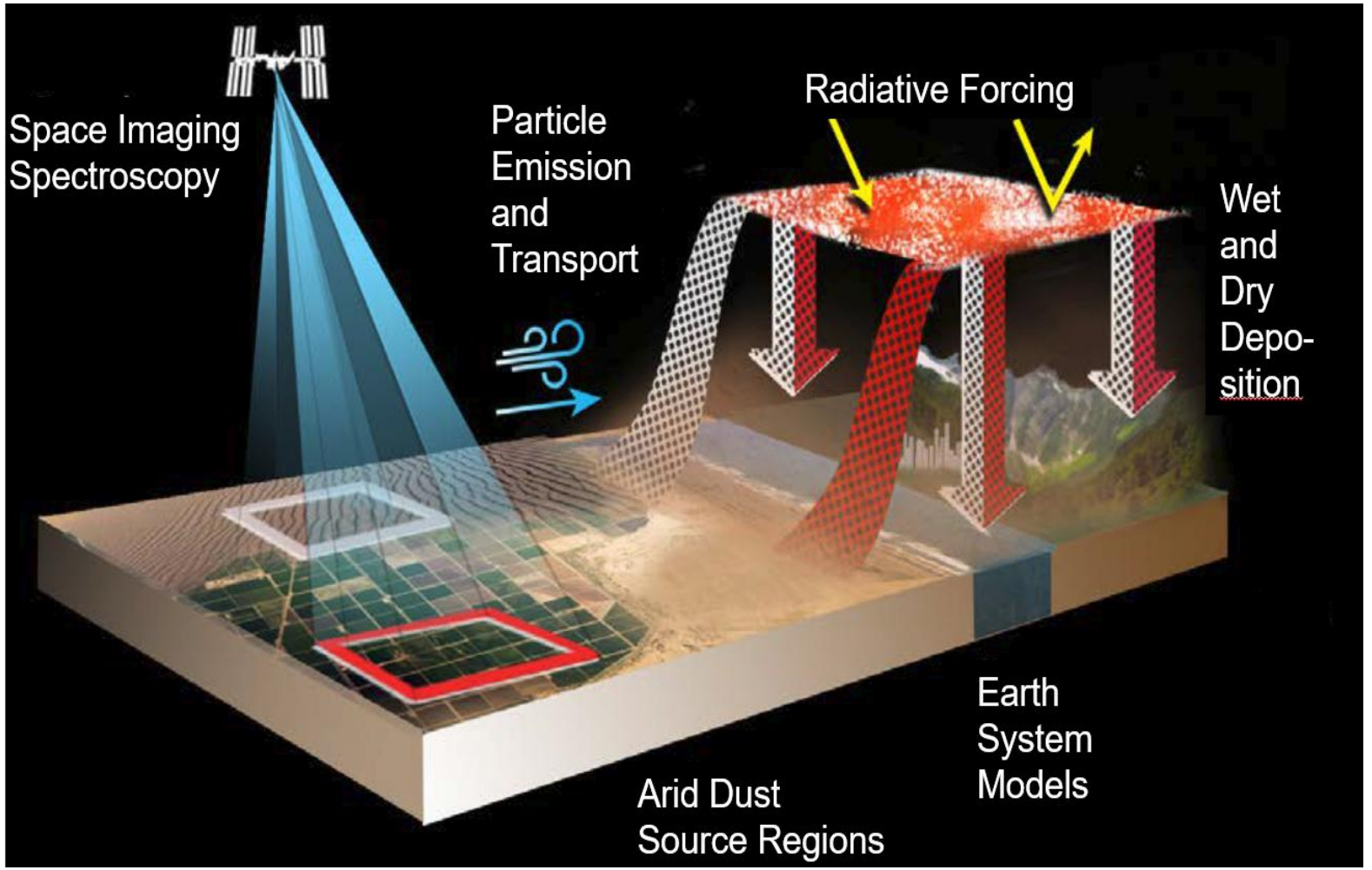

The Earth surface Mineral dust source InvesTigation

Retrieved Surface Reflectance and Uncertainty

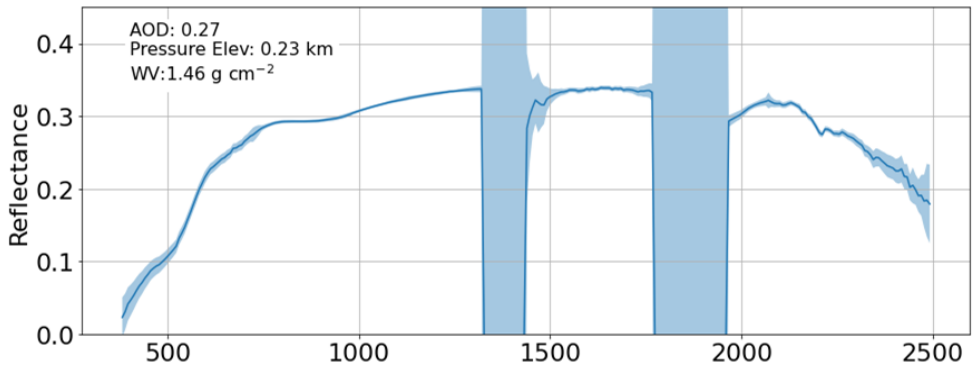

Thompson et al, 2018

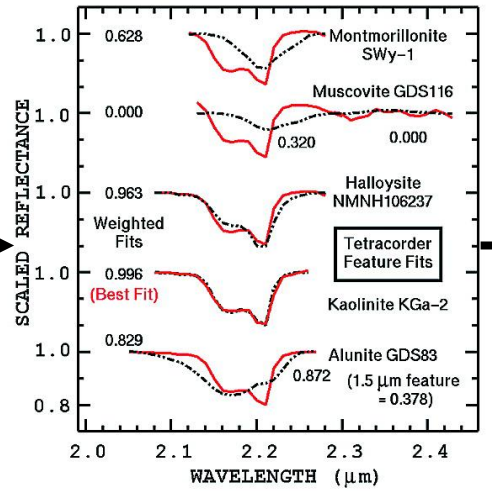

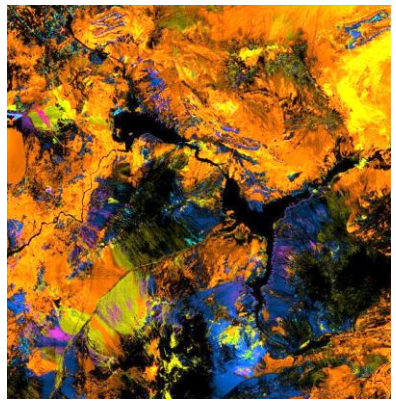

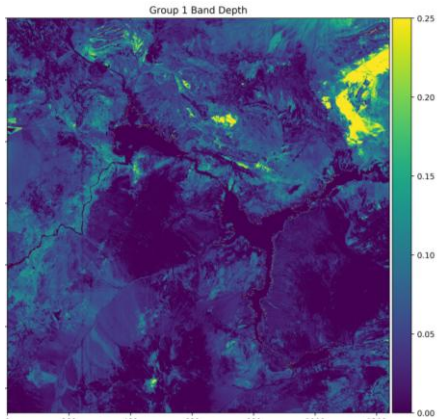

Clark et al, 2003

Quantitative **Mass Fraction**
Abundance (and uncertainty)

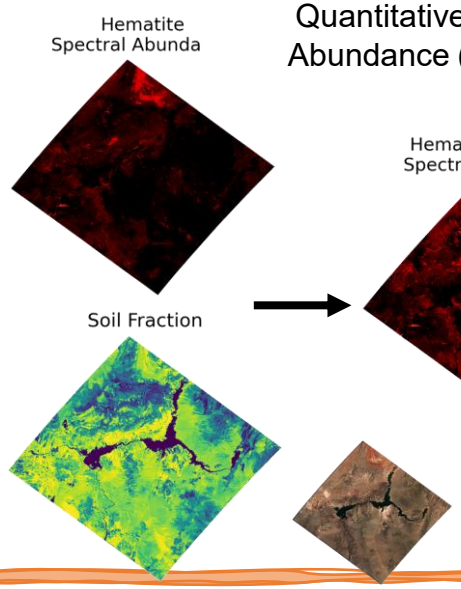

Spatial Aggregation

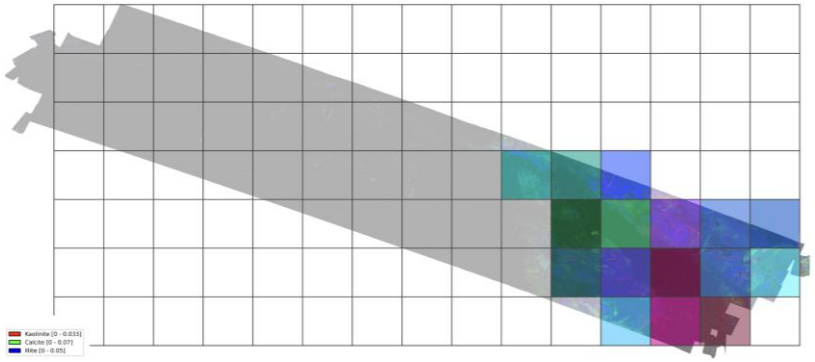

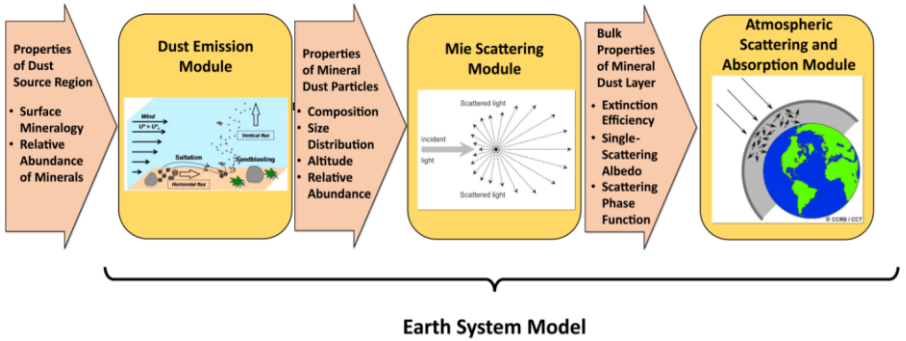

Ochoa et al, *In Prep*
Clark et al, 2003

Individual minerals

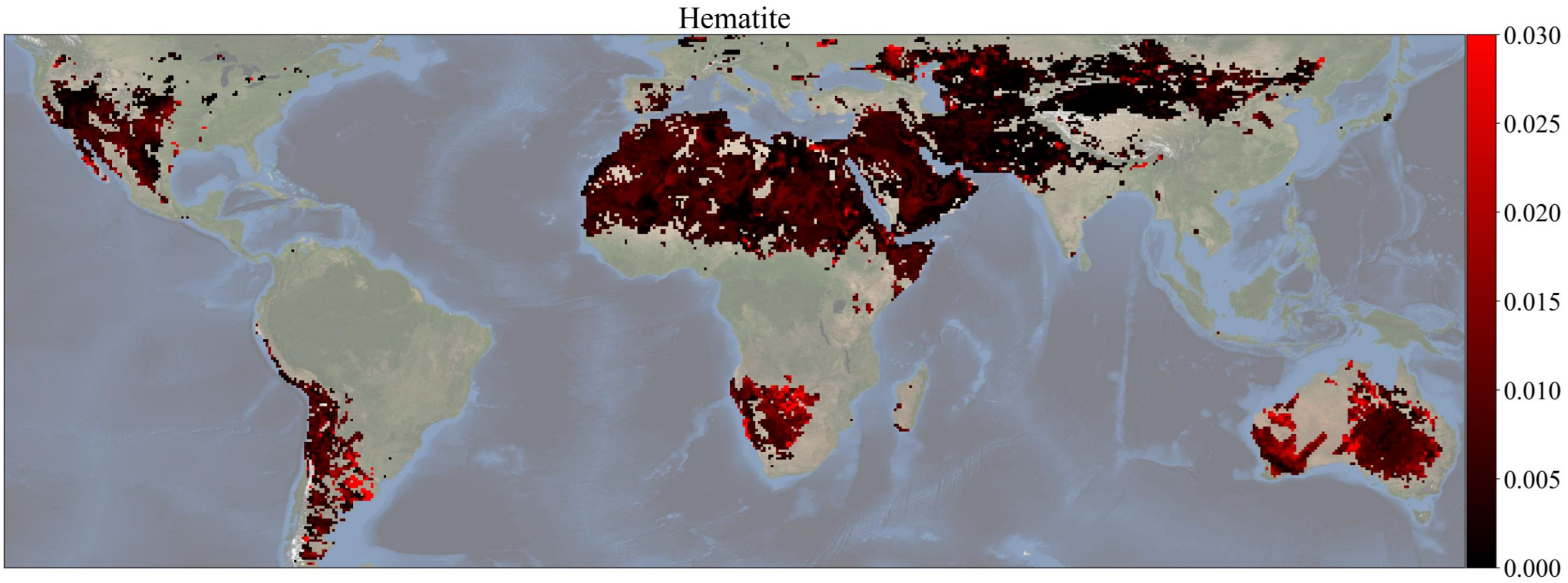

Individual minerals

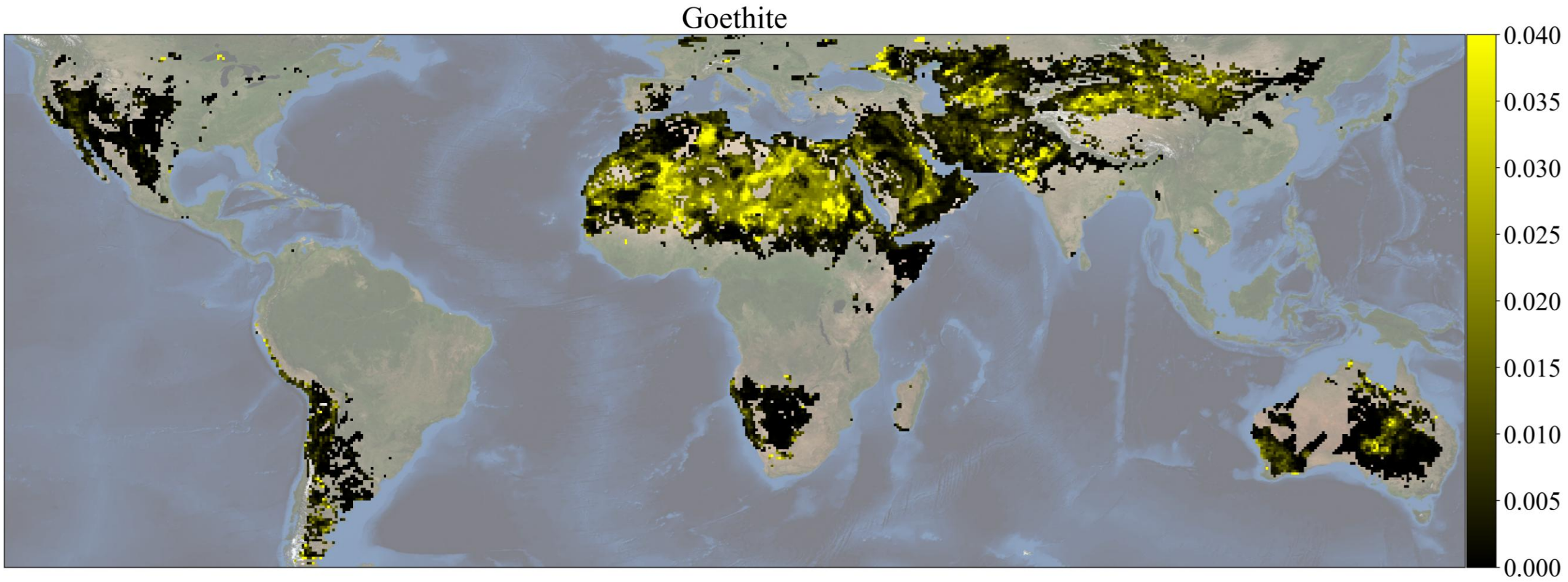

Individual minerals

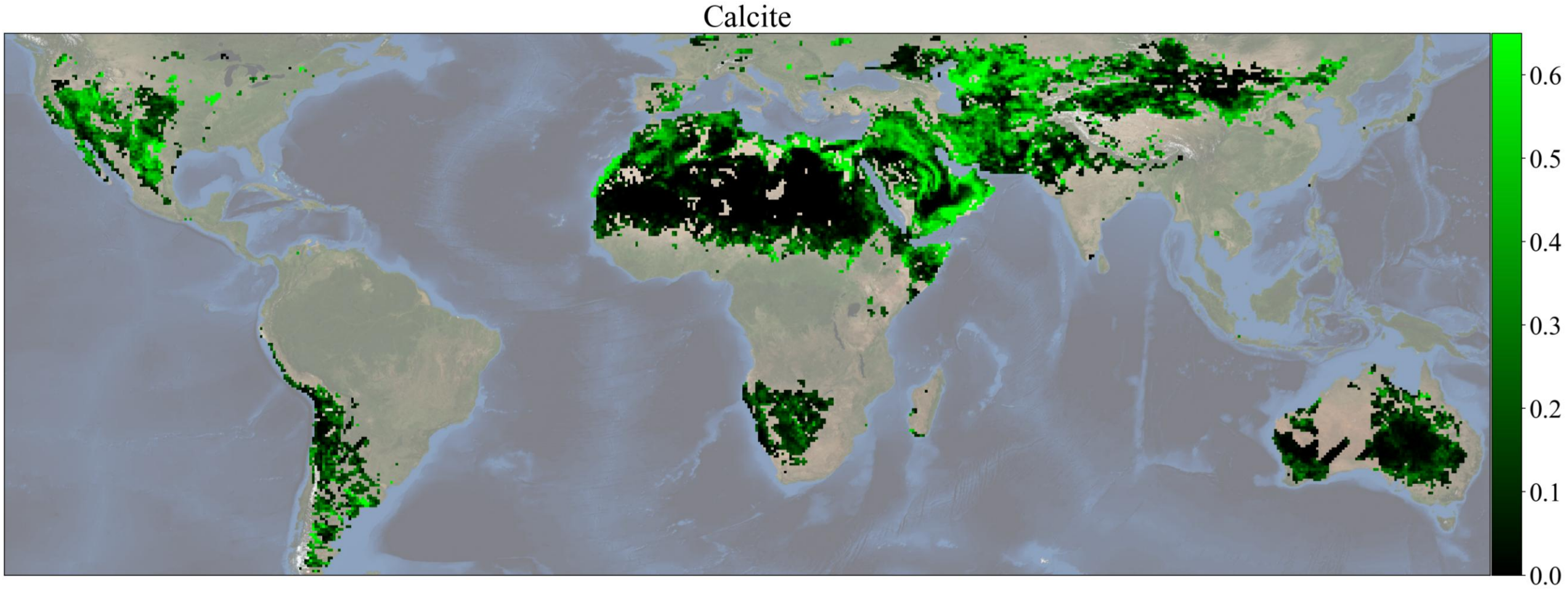

Background and Definitions

Direct Radiative Effect (DRE)

Atmospheric dust aerosols scatter and absorb shortwave (SW) and longwave (LW) radiation:

The dust DRE is the instantaneous change of the radiative balance due to aerosols:

$$R = (F_d - F_u)_a - (F_d - F_u)_o$$

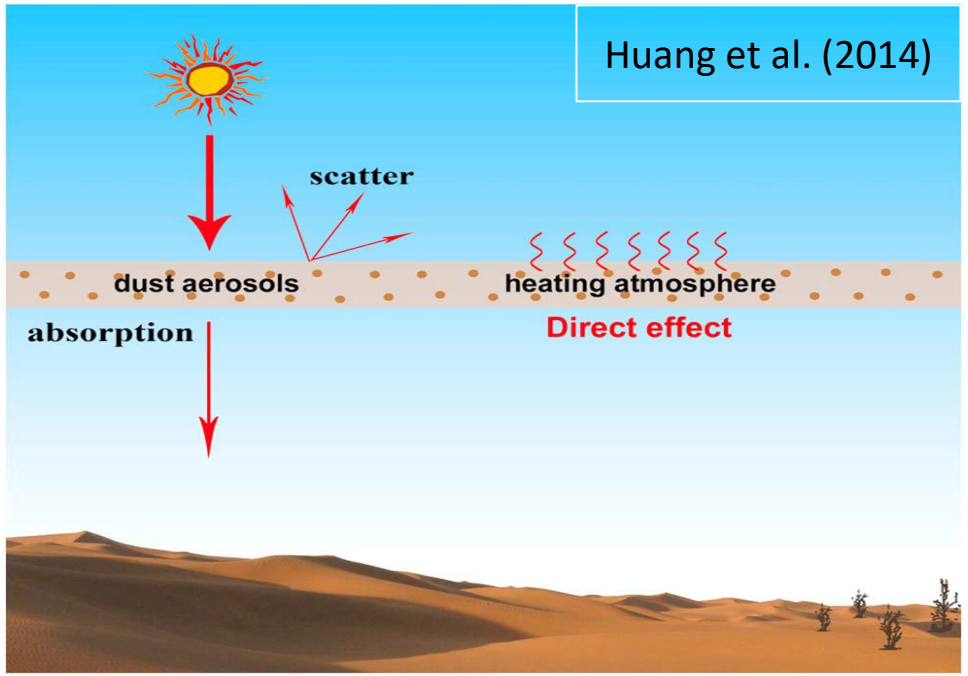

Background and Definitions

Dust optical properties

Models typically represents dust-radiation interaction through 3 optical properties:

Dust Optical Depth (DOD): $\tau > 0$

Single-Scattering Albedo (SSA): $0 < \omega < 1$

Asymmetry Parameter (ASY): $-1 < g < 1$

DOD quantifies the attenuation of radiation due to scattering and absorption by dust layers.

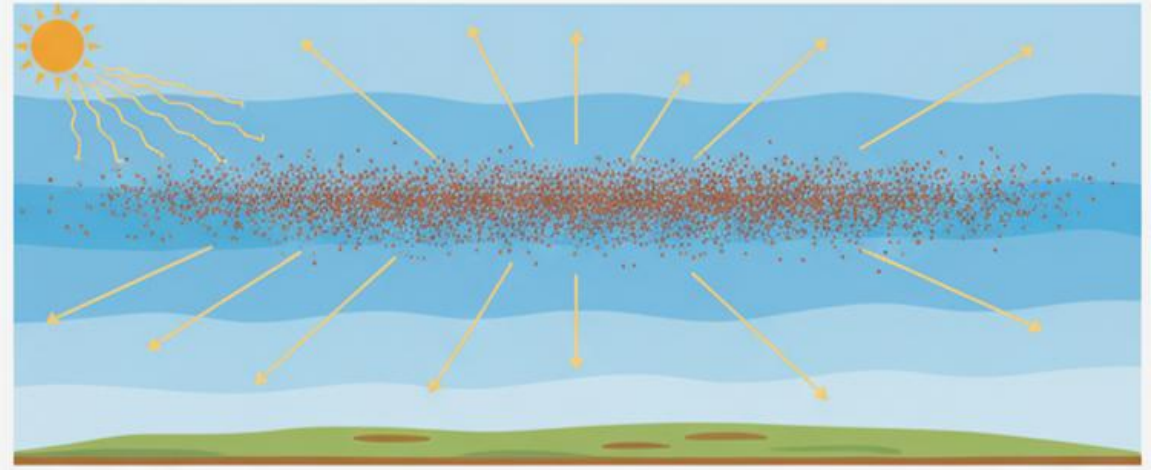

Background and Definitions

Dust optical properties

Models typically represents dust-radiation interaction through 3 optical properties:

Dust Optical Depth (DOD): $\tau > 0$

Single-Scattering Albedo (SSA): $0 < \omega < 1$

Asymmetry Parameter (ASY): $-1 < g < 1$

SSA quantifies the fraction of scattered radiation with respect to the total extinct radiation.

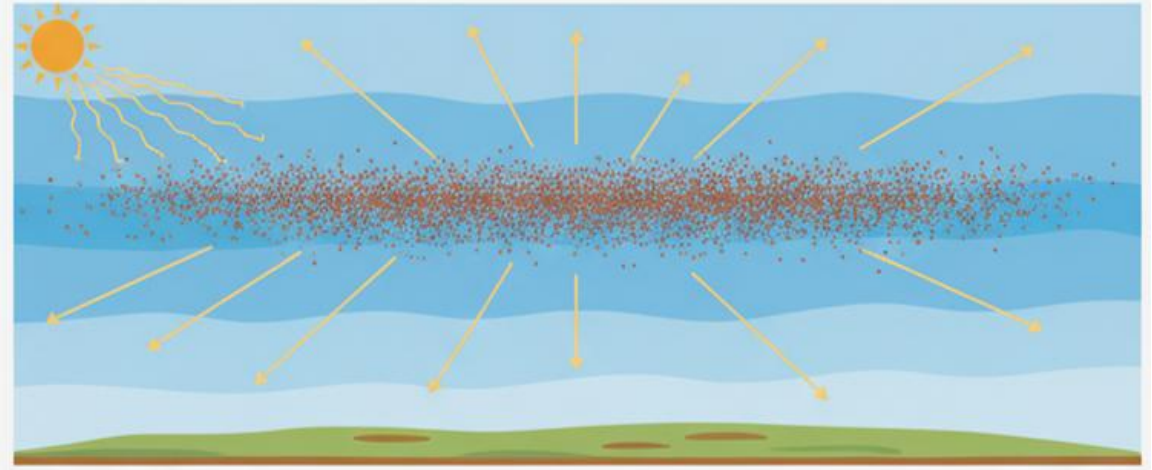

Background and Definitions

Dust optical properties

Models typically represents dust-radiation interaction through 3 optical properties:

Dust Optical Depth (DOD): $\tau > 0$

Single-Scattering Albedo (SSA): $0 < \omega < 1$

Asymmetry Parameter (ASY): $-1 < g < 1$

ASY measures the dominant semi-integral direction of scattering (backward vs. forward).

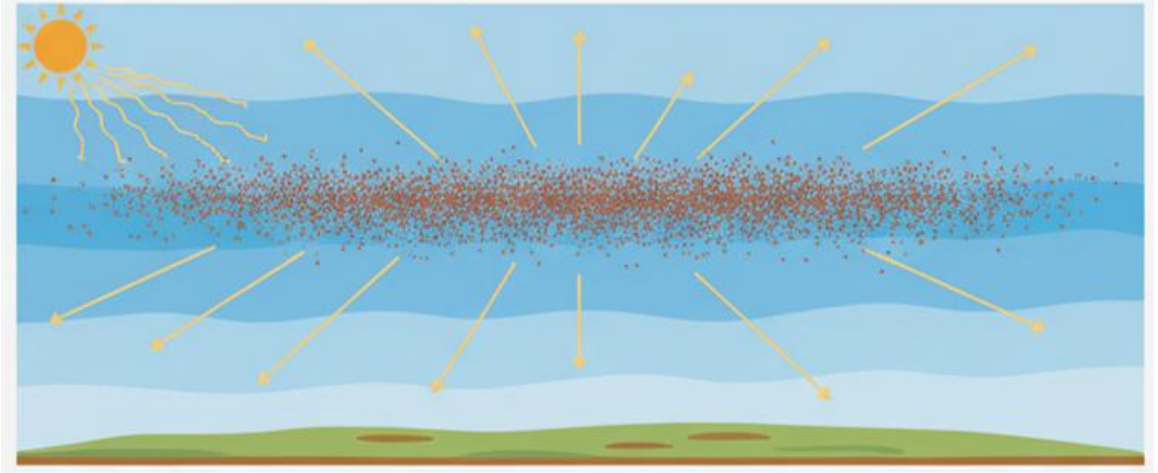

Background and Definitions

Dust physical properties

Optical properties are calculated with scattering codes taking particle physical properties as inputs:

Size parameter: $x = \pi d/\lambda$

Complex refractive index (CRI): $\tilde{n} = n + ik$

Dust particle shape

Bulk optical properties are functions of the particle size distribution (PSD) and spectral bands.

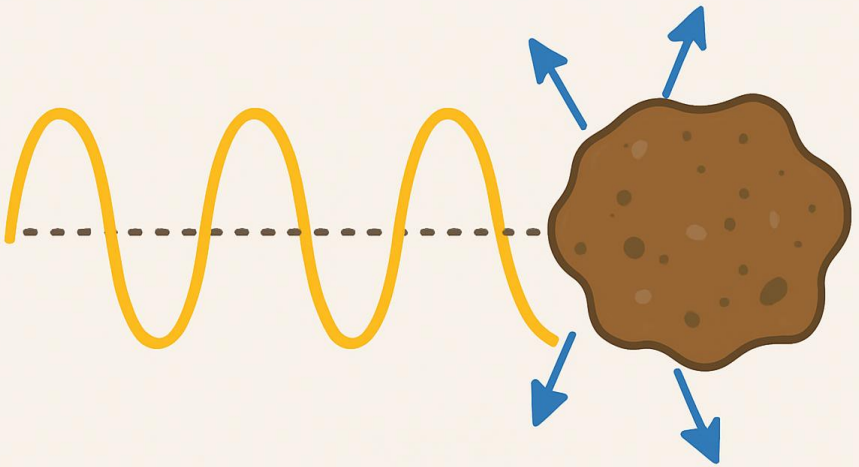

Background and Definitions

Dust physical properties

Optical properties are calculated with scattering codes taking particle physical properties as inputs:

Size parameter: $x = \pi d/\lambda$

Complex refractive index (CRI): $\tilde{n} = n + ik$

Dust particle shape

CRI is defined by the mineral composition: imaginary part (IRI) determines the absorption.

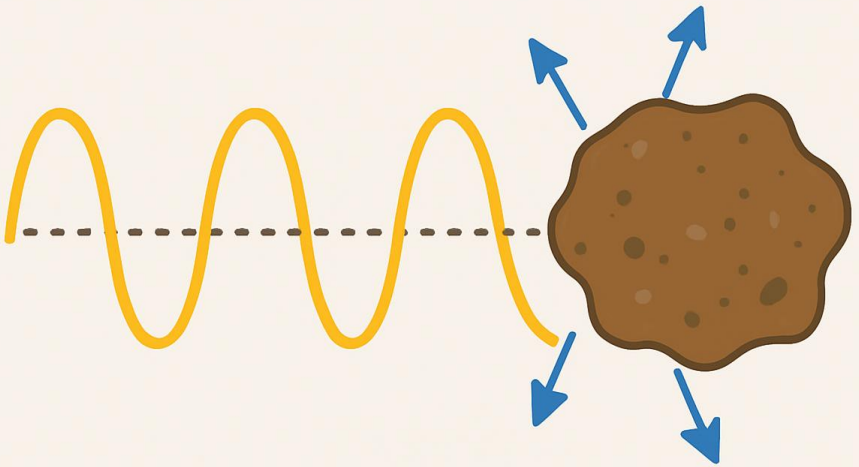

Background and Definitions

Dust physical properties

Optical properties are calculated with scattering codes taking particle physical properties as inputs:

Size parameter: $x = \pi d/\lambda$

Complex refractive index (CRI): $\tilde{n} = n + ik$

Dust particle shape

Typically spherical shape is assumed for dust; higher asphericity approximates irregular shapes.

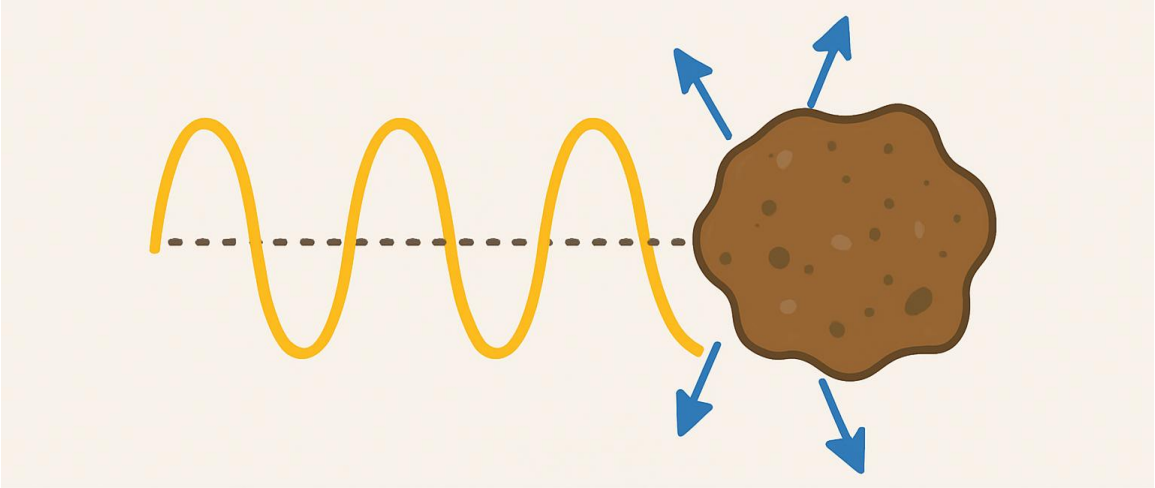

Modeling Challenges

Uncertainty affecting all aspects of dust physical representation is a key challenge to an accurate modeling of dust-radiation interaction in climate models.

I. PARTICLE SIZE DISTRIBUTION	II. COMPLEX REFRACTIVE INDEX	III. DUST PARTICLE SHAPE
• Uncertain dust-cycle processes • Underestimated coarse dust	• Soil mineralogy of dust sources • Mixing of mineral indices	• Global shape distributions • Non-spherical scattering data

Particle Size Distribution

Uncertain dust-cycle processes

Emission, transport, dry and wet deposition determine mass size distribution in model simulations.

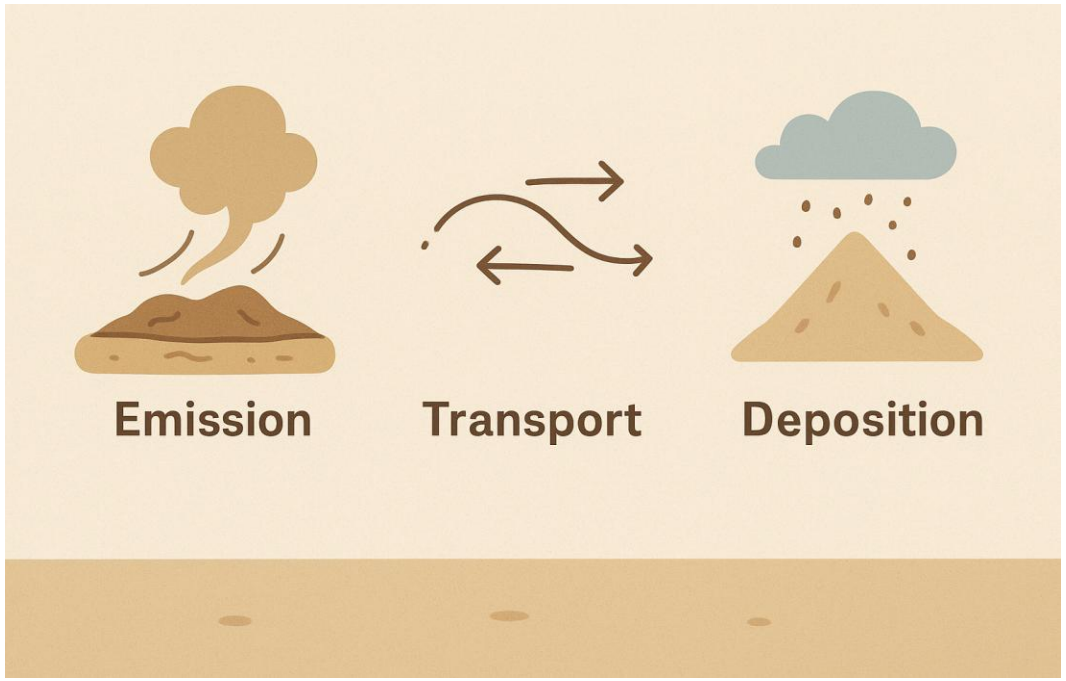

Particle Size Distribution

Underestimated coarse dust

Using observational constraints, Adebiyi and Kok (2020) showed that models underestimate coarse dust:

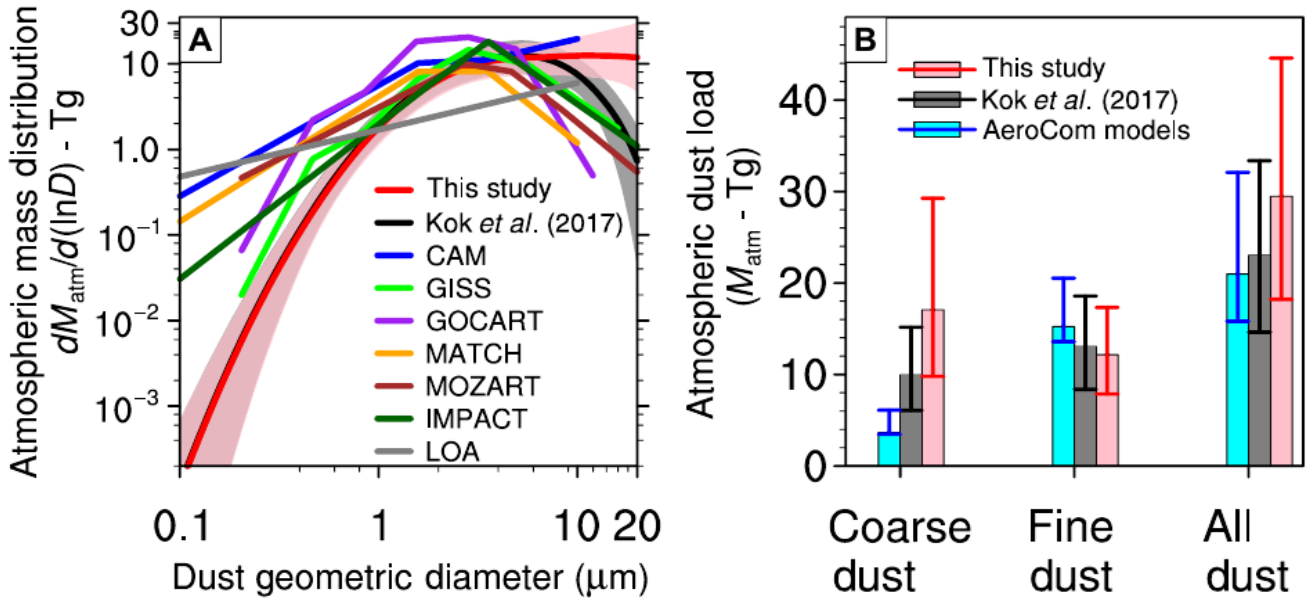

Complex Refractive Index

Soil mineralogy of dust sources

Iron oxides are key minerals because absorb solar radiation (Di Biagio et al., 2019: DB19).

Complex Refractive Index

Soil mineralogy of dust sources

Traditional soil maps rely on a limited number of observations (Claquin et al., 1999; Journet et al., 2014).

NASA EMIT Mission (Green et al., 2023)

- Imaging spectroscopy from ISS.
- Surface reflectances (VIS-NIR).
- Spectral signatures of minerals.
- Soil mineralogy from spectral abundances.
- Spatial aggregation to model resolution.

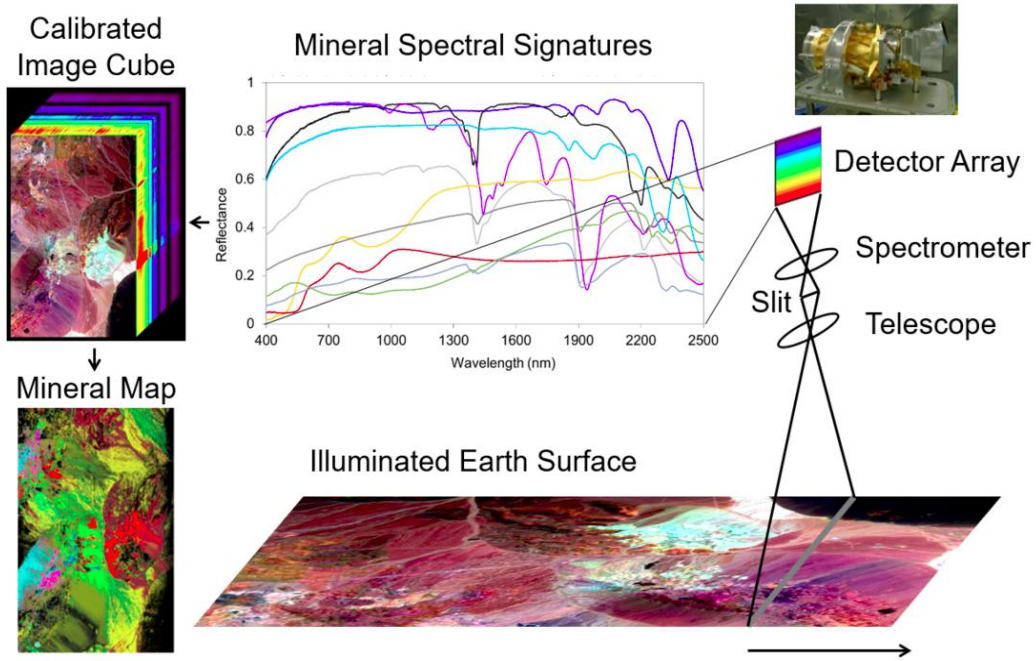

Complex Refractive Index

Mixing of mineral indices

Estimates of imaginary index of iron oxides from the literature are strongly uncertain (Zhang et al., 2015):

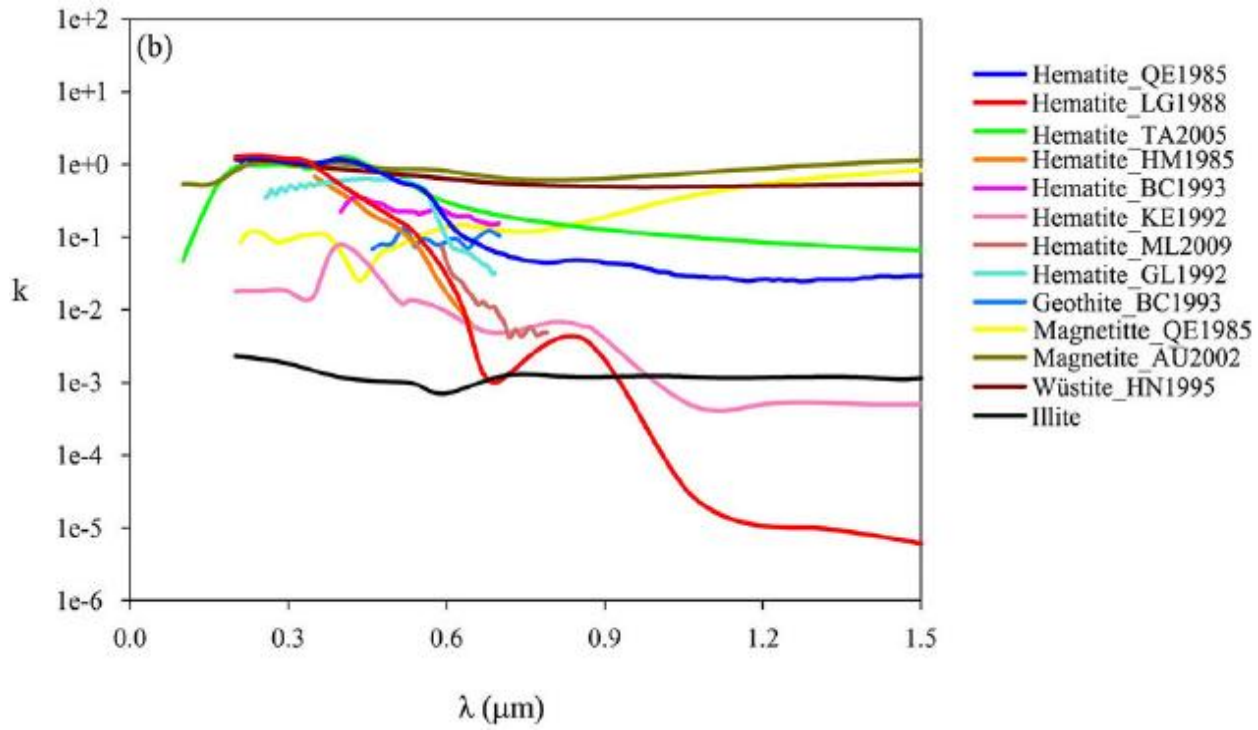

Complex Refractive Index

Mixing of mineral indices

Empirical relationships of dust imaginary index to iron oxides allows new estimates (Di Biagio et al., 2019):

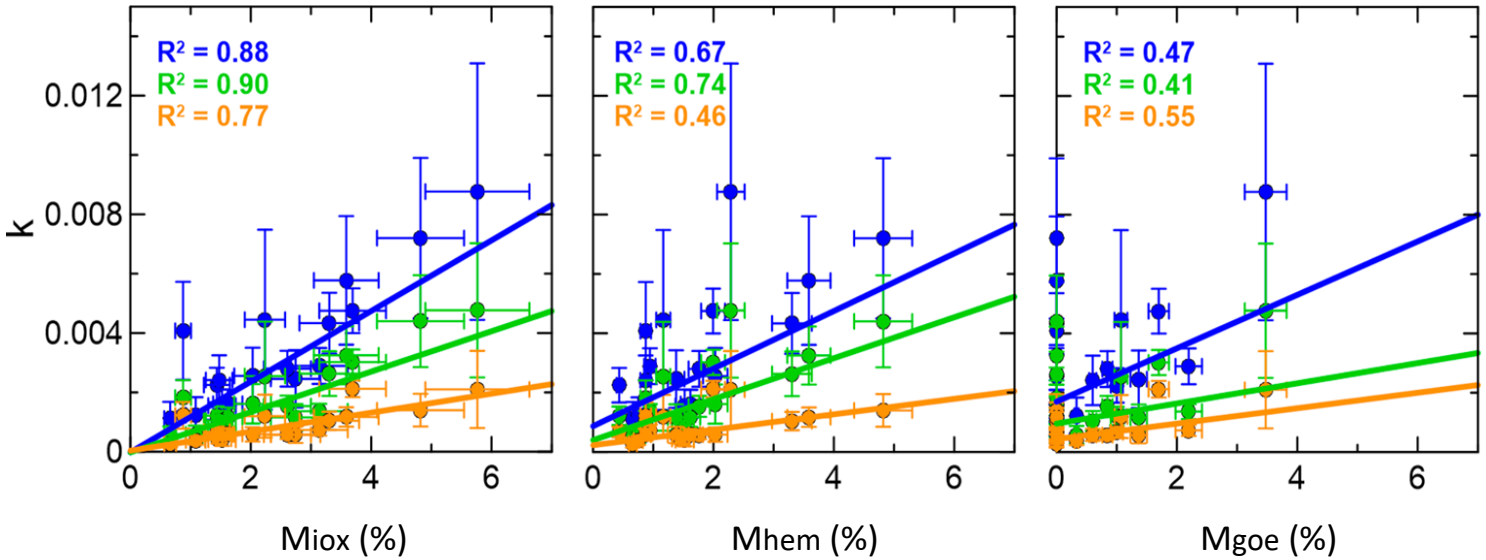

Dust Particle Shape

Global shape distributions

Natural dust particles are observed to have strongly irregular shapes (Kalashnikova and Sokolik, 2004):

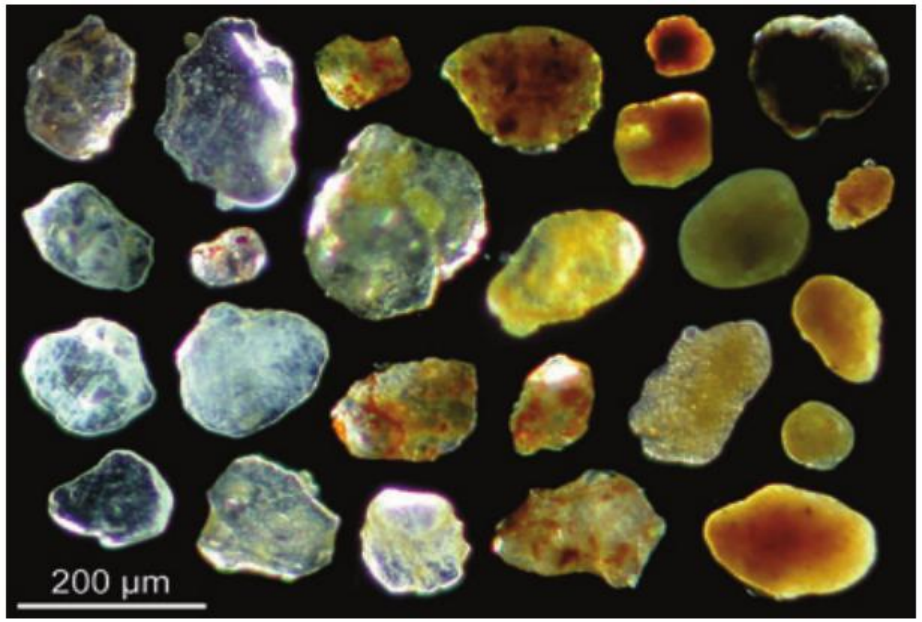

Kandler et al. (2009)

Dust Particle Shape

Global shape distributions

Globally representative ellipsoid distributions were fitted to observed shapes (Huang et al., 2020: HG20):

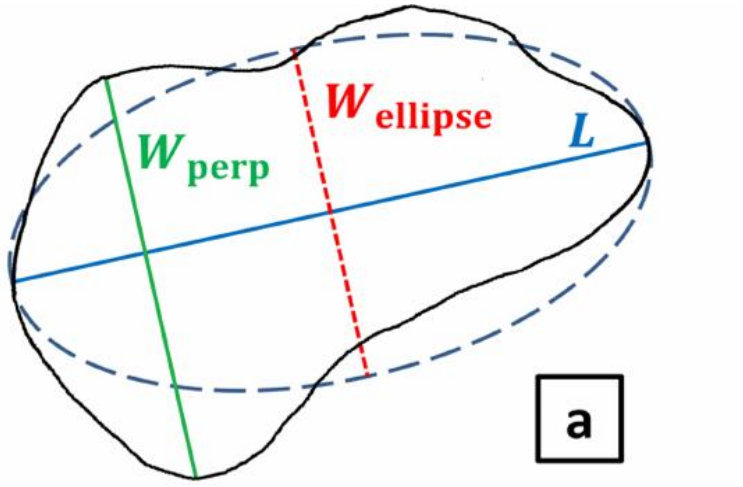

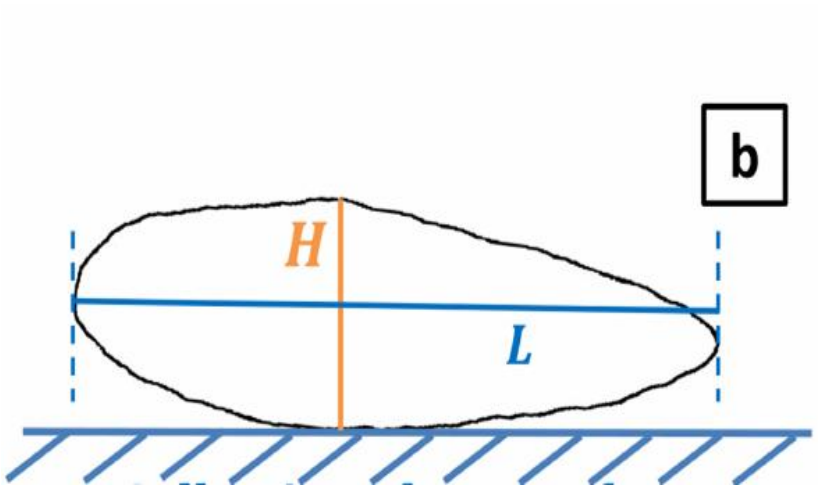

Dust Particle Shape

Non-spherical scattering databases

Shape models of increasing complexity have been developed for remote sensing and model applications:

SPHEROIDS (e.g., Dubovik et al., 2006)	ELLIPSOIDS (Meng et al., 2010: MG10)	HEXAHEDRONS (Saito et al., 2021: ST21)

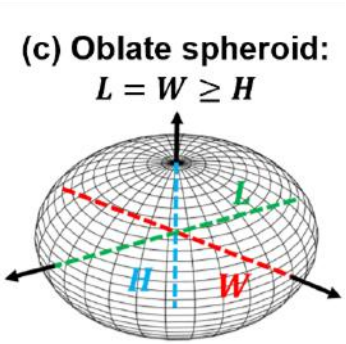

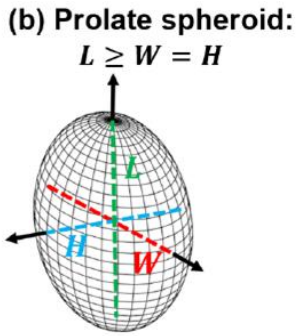

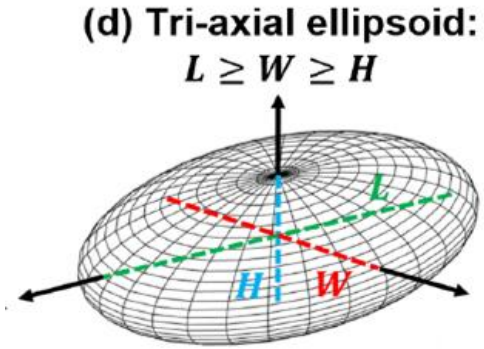

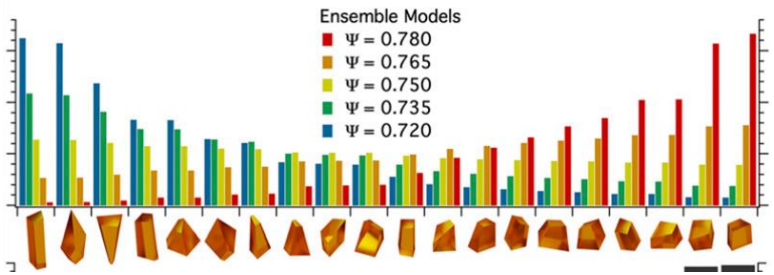

INCREASING SHAPE COMPLEXITY

Dust Particle Shape

Effect of non-sphericity on dust optical properties (Obiso et al., in rev.)

Ellipsoids (MG10) globally distributed according to observations (HG20) primarily increases extinction:

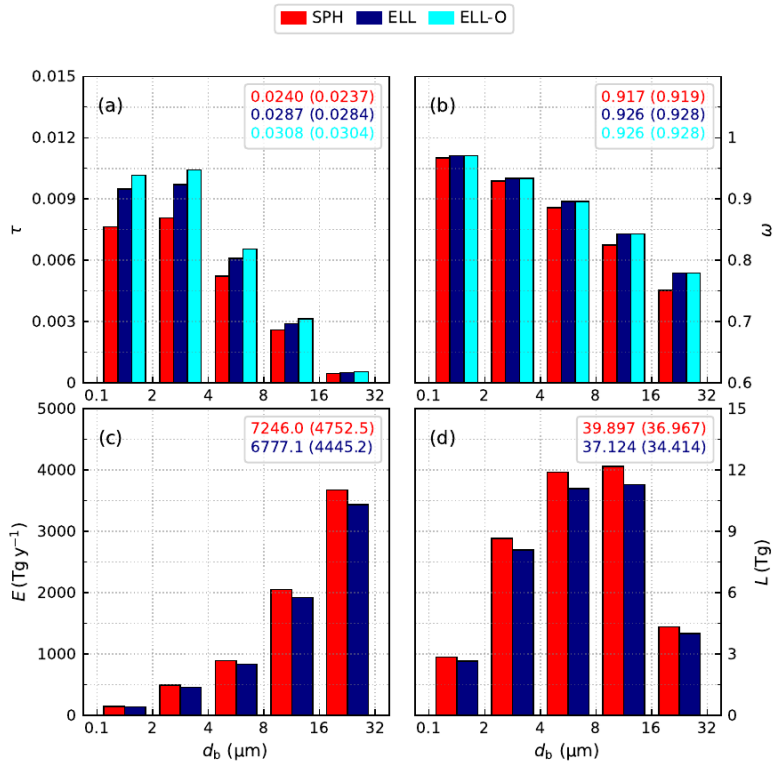

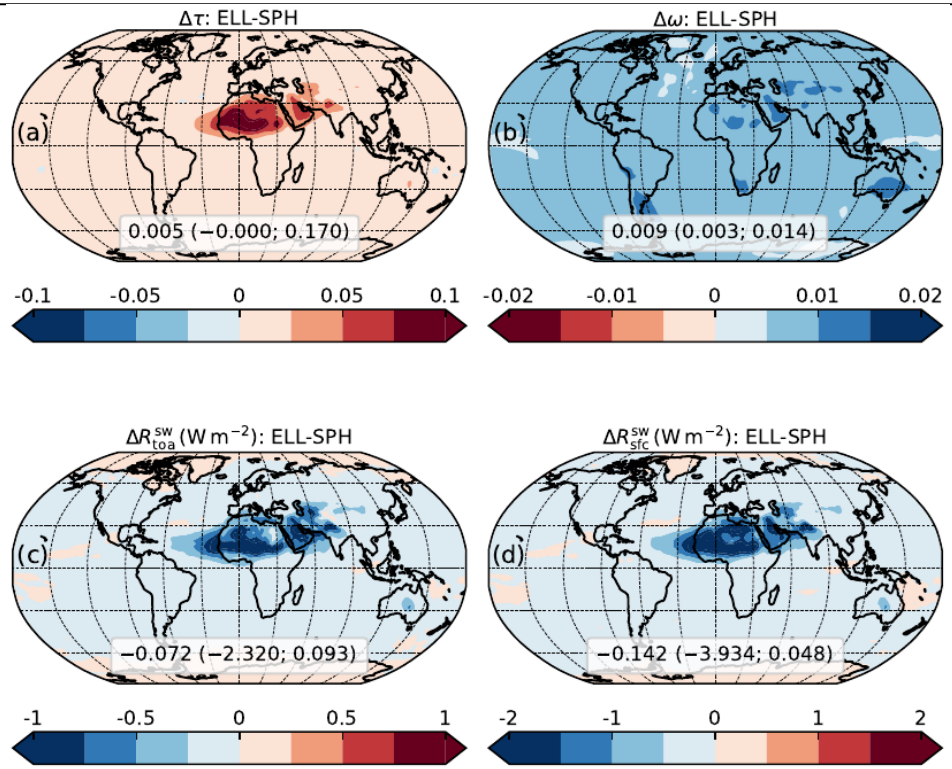

Assessment of dust SSA (Obiso et al., in prep.)

We merge as many observational constraints as possible into model calculations to improve the representation of dust-radiation interaction for climate applications.

I. PARTICLE SIZE DISTRIBUTION

- Retrieved PSD from AERONET
- Constrained PSD from DustCOMM
- Modeled PSD from MONARCH

II. COMPLEX REFRACTIVE INDEX

- Soil mineralogy from EMIT
- Host mixture (Scanza et al., 2015)
- IRI of iron oxides from DB19

Particle Size Distribution

All PSDs mapped onto common bins

AERONET (Sinyuk et al., 2020):
Retrieved column particle volume in 22 bins: d = 0.1 - 30 µm.

DustCOMM (Adebiyi et al., 2020)
Constrained column mass load in 9 bins: d = 0.2 - 100 µm.

MONARCH (Pérez et al., 2011; Gonçalves et al., 2023)
Modeled column mass load in 8 bins: d = 0.2 - 20 µm.

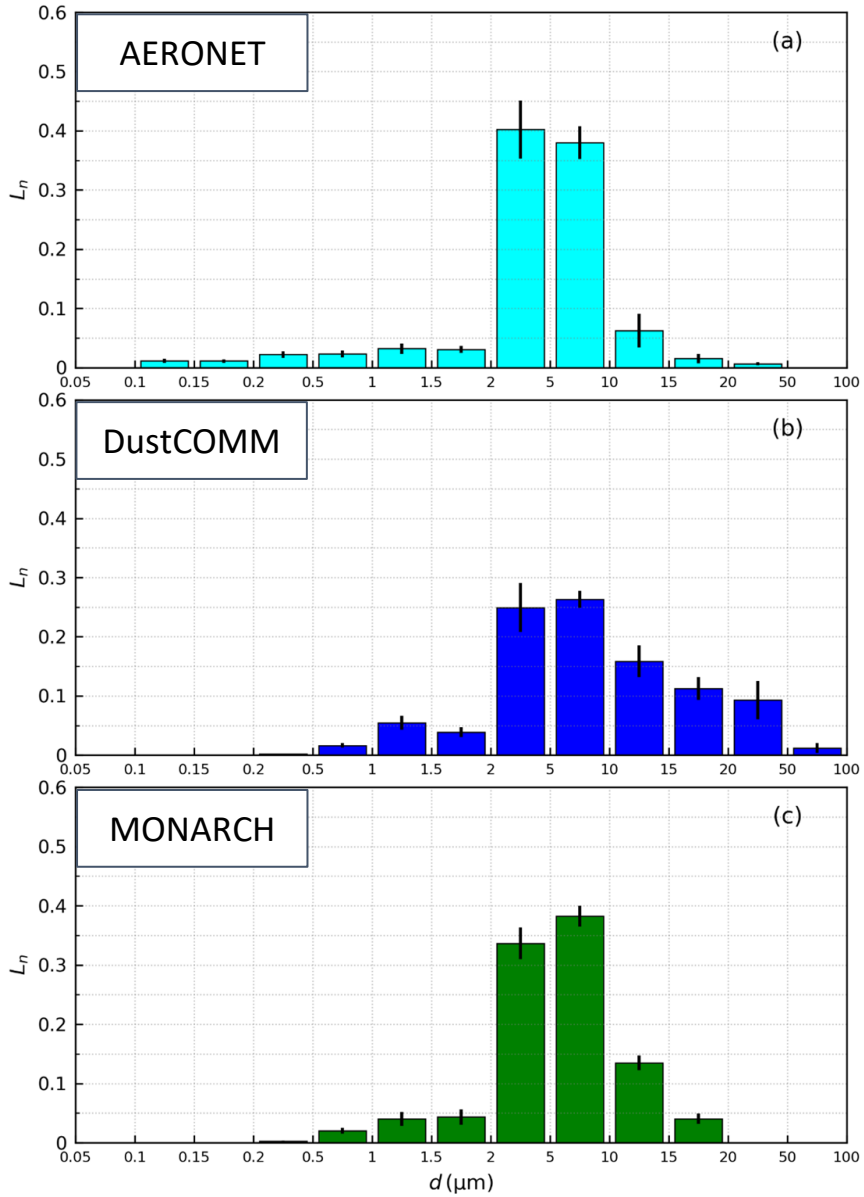

Complex Refractive Index

EMIT soil mineralogy

All minerals lumped into:
host + hematite + goethite

https://earth.jpl.nasa.gov/emit/

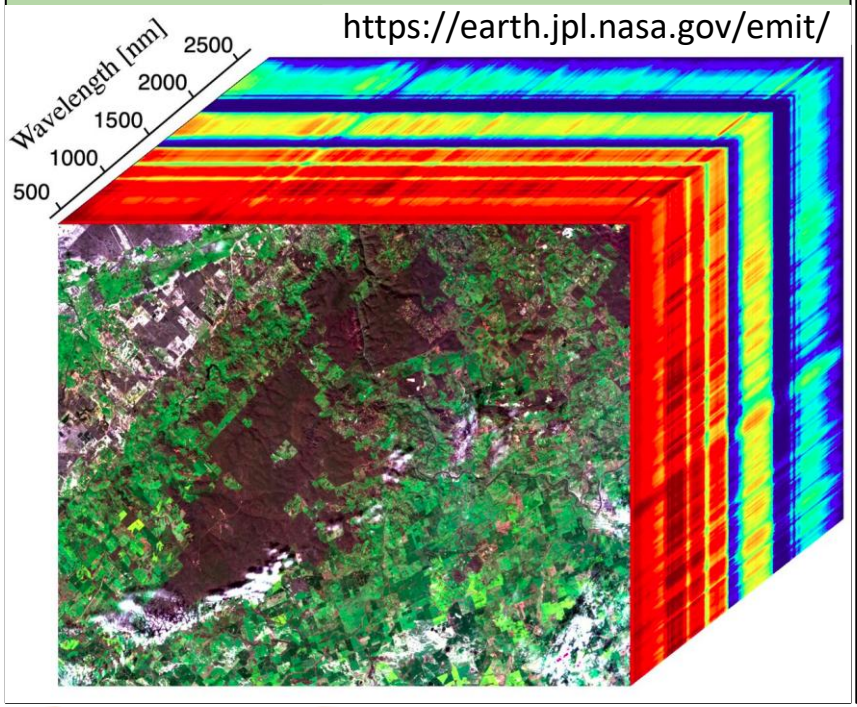

Host amalgam

Globally uniform CRI:
$\tilde{n}_h = \sum_j \tilde{n}_j v_j$

Scanza et al. (2015)

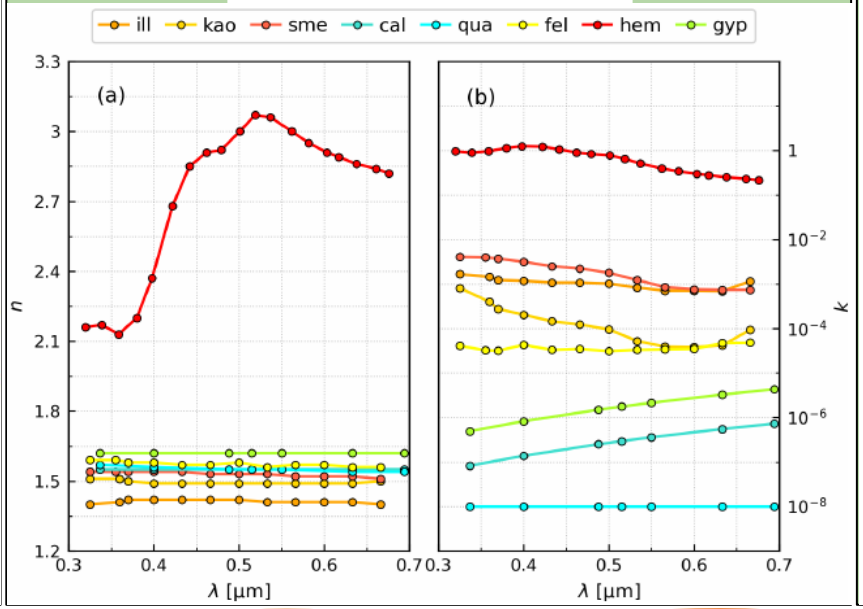

Iron oxides

Inversion of DB19 data:
$k_{db} = k_h + S(\tilde{n}_h, \tilde{n}_i)\, v_{db}$

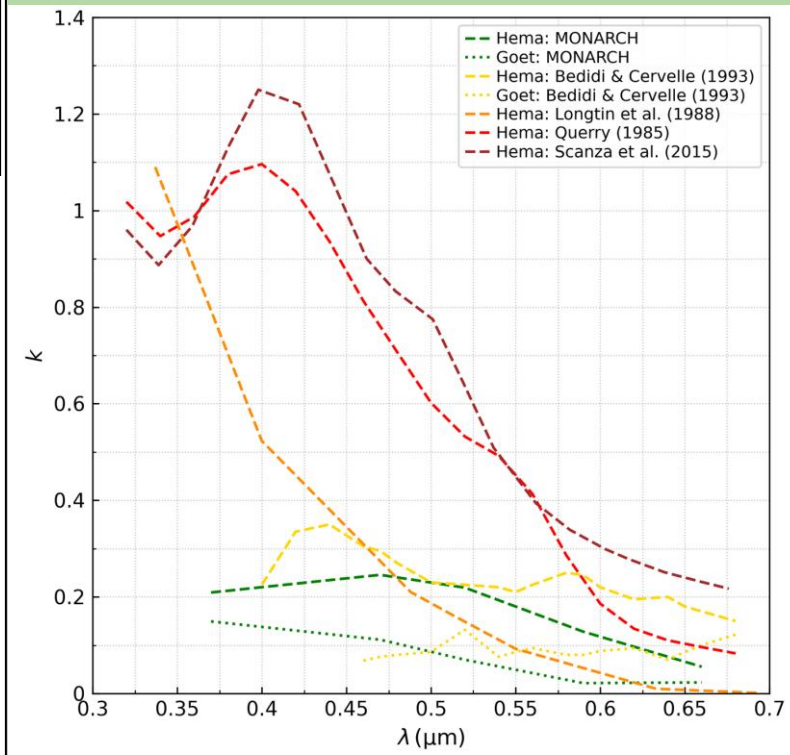

Aeronet Selected Retrievals

Climatological monthly means

Strict filtering conditions identify dusty scenes (Obiso et al., 2024; Gonçalves et al., 2023):

Filtering conditions
(Dubovik et al., 2002; Schuster et al., 2016)

- Fine-volume fraction: $v_f < 0.10$
- Single-scattering albedo: $\omega_{675} > \omega_{440}$
- Mean imaginary index: $k_{675\text{-}870\text{-}1020} < 0.0042$

Months with 80+ measurements: 27 stations (x) in 6 dust regions.

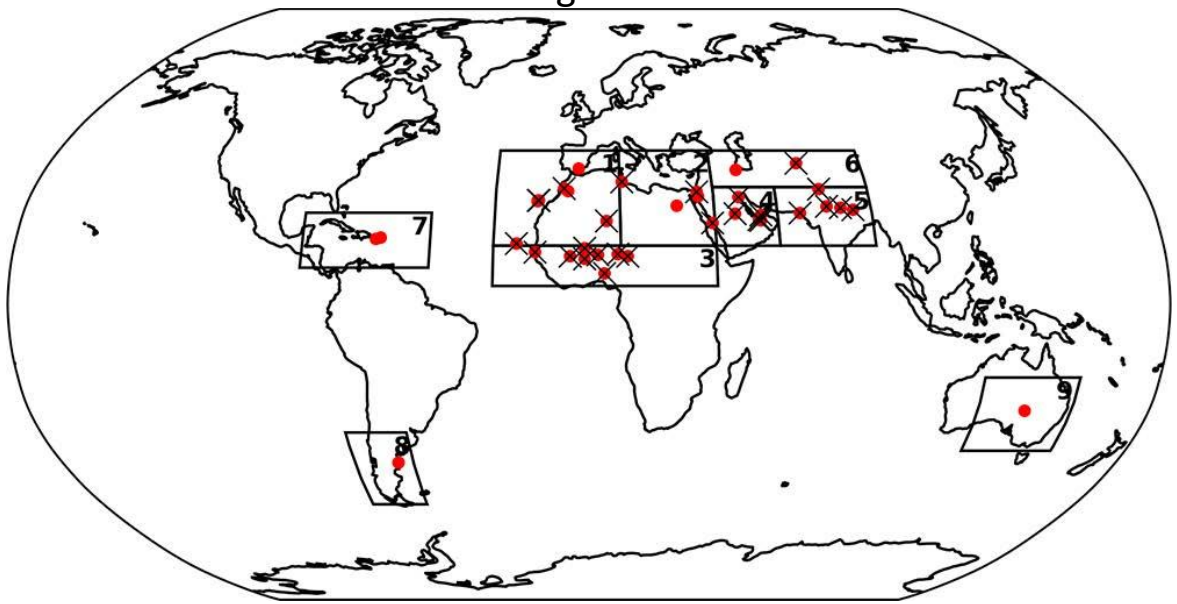

Seasonal SSA in VIS band

AERONET PSD + EMIT-based uniform (a) and varying (b) IRI

Regionally varying IRI increases the spread of dust absorption but “fine” PSD leads to overestimated SSA.

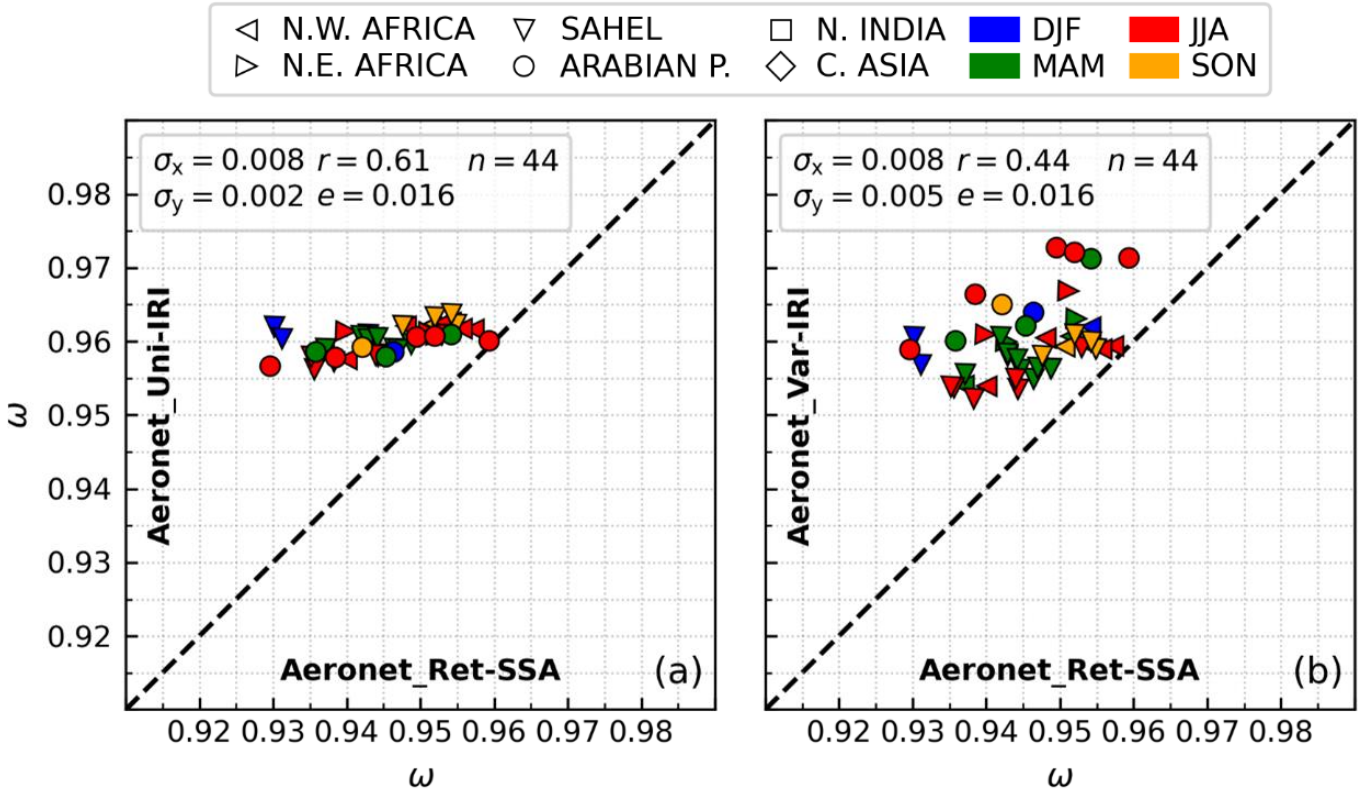

Seasonal SSA in VIS band

MONARCH PSD + EMIT-based uniform (a) and varying (b) IRI

EMIT-based varying IRI increases spread, more consistent with observations, and improves correlation.

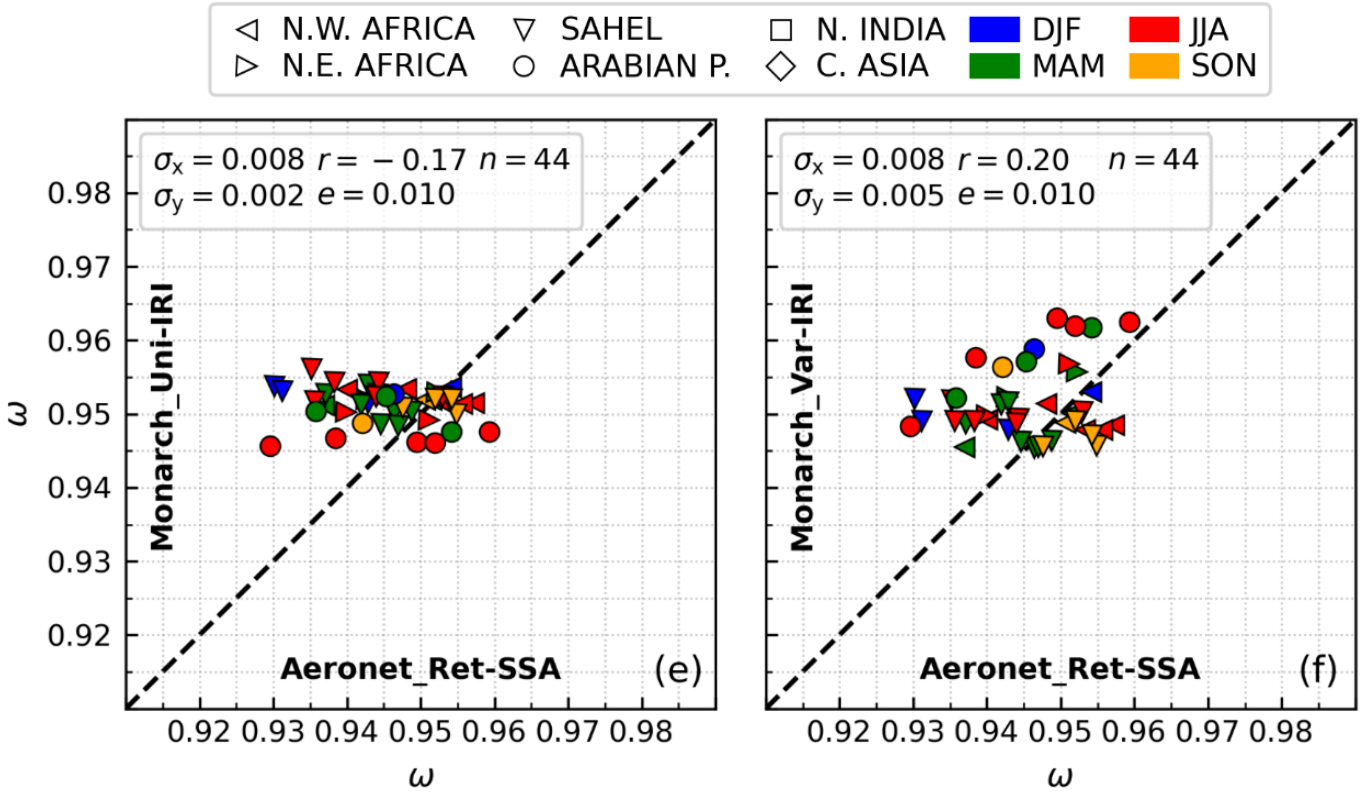

Seasonal SSA in VIS band

DustCOMM PSD + EMIT-based uniform (a) and varying (b) IRI

Varying IRI doubles correlation (already good with constrained PSD) and giant dust improves comparison.

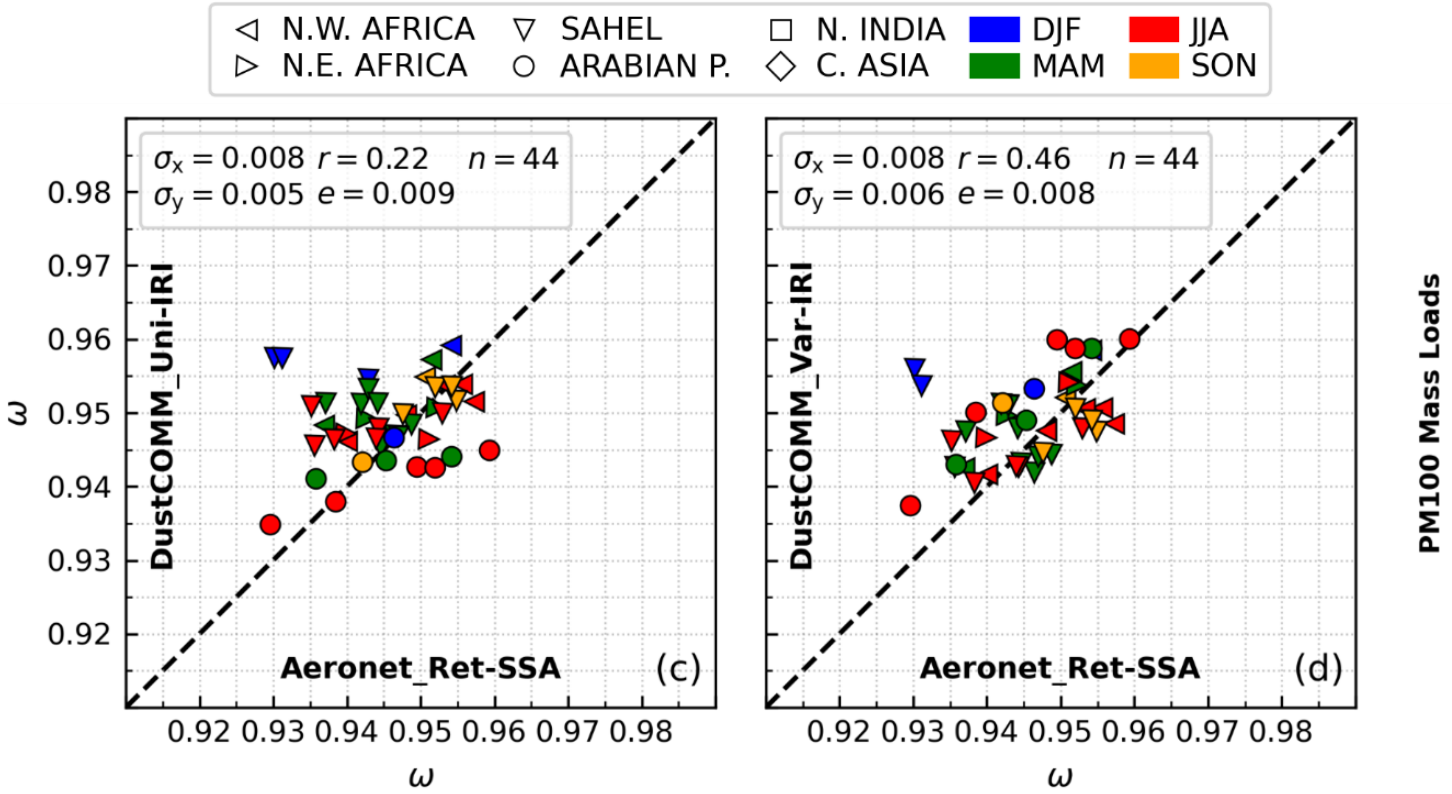

Remaining uncertainties

PARTICLE SIZE DISTRIBUTION

- Most models still miss particles beyond 20 µm, whose impact appears to be important to dust SSA.
- Model dust-cycle processes are uncertain: hybrid calculations using constrained PSD may help.

COMPLEX REFRACTIVE INDEX

- Constraints on mineral CRIs from DB19 are limited by assumptions: spherical shape and bulk mineralogy.
- AERONET observations include non-dust species (despite filtering): small contamination may affect SSA.

DUST PARTICLE SHAPE

- Ellipsoidal scattering data from MG10 are incomplete according to HG20 (Obiso et al., in rev.).
- More complex shapes (e.g., hexahedrons) lack in globally representative distributions based on observations.

Impact of dust-radiation interactions on weather forecasting

8-15 April 2002 major dust outbreak over the Mediterranean

2 sensitivity experiments

CTR

dust is considered as a dynamic tracer without interaction with atmospheric radiation

RAD

interaction between short- and long-wave radiation and dust is included

- ✓ Cold Start on 5 April 2002
- ✓ 50 km horizontal resolution
- ✓ 24 layers up to 15 km vertical

MSL pressure 12 April at 12 UTC

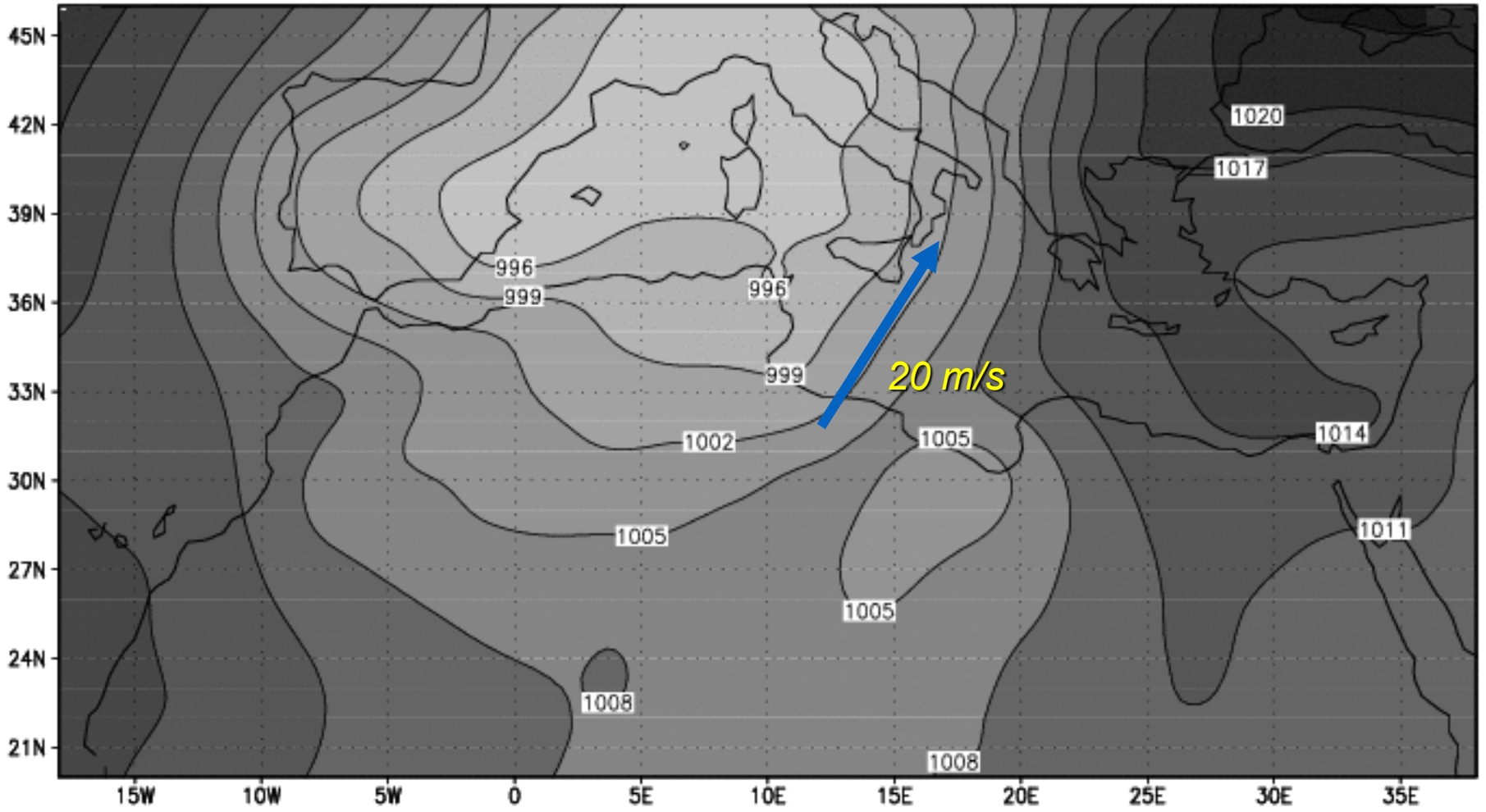

Pérez et al. (2006)

Comparison with observations

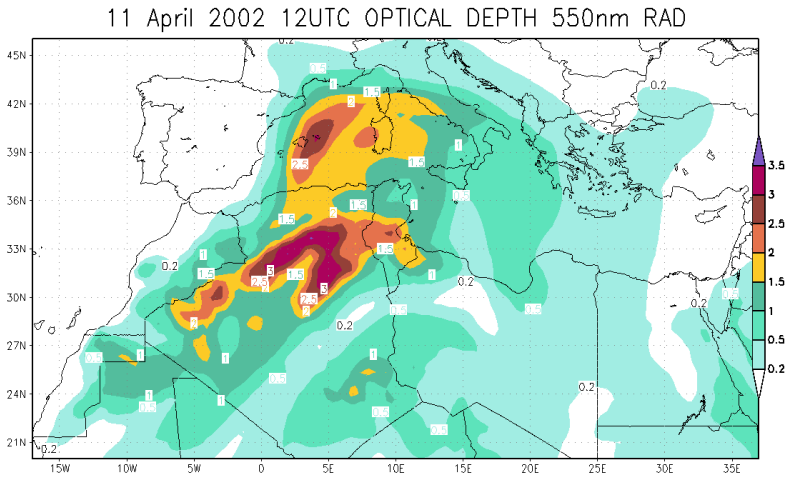

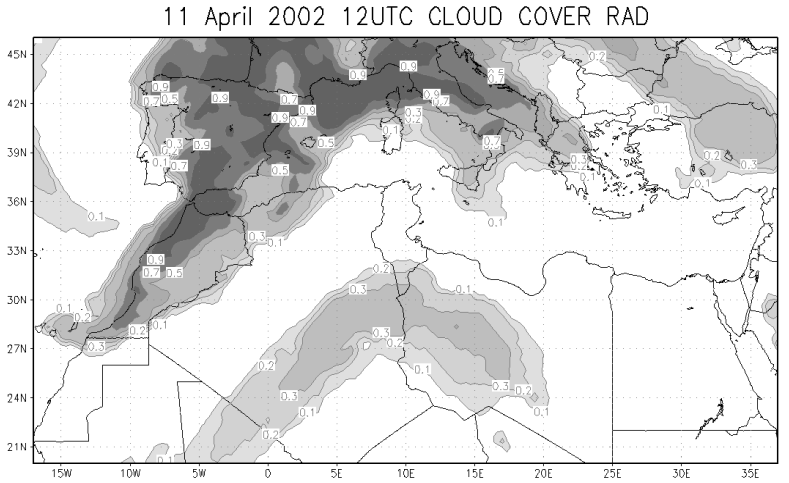

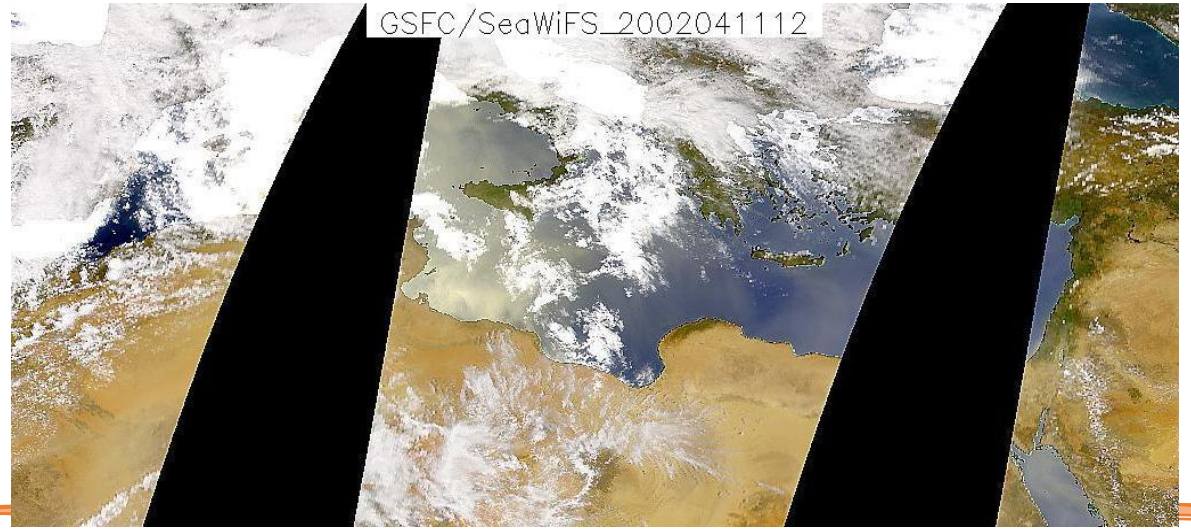

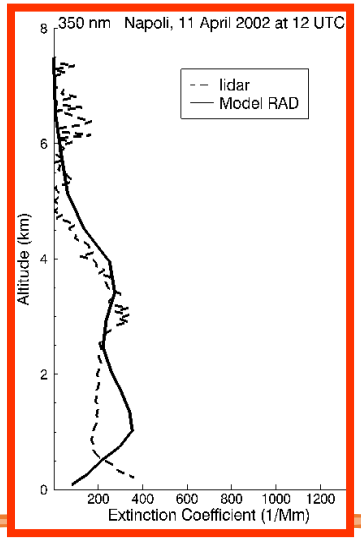

Napoli Raman Lidar

Comparison with observations

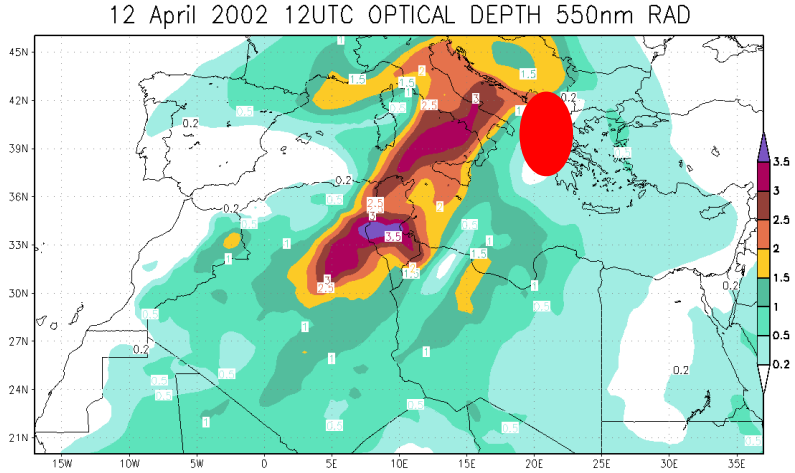

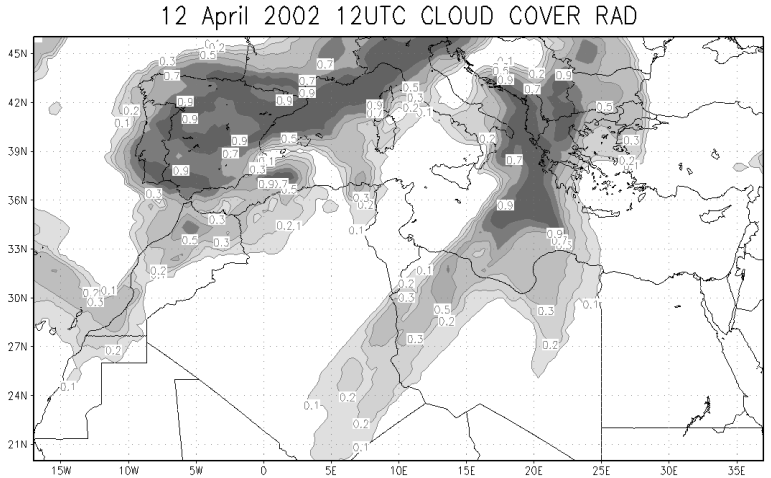

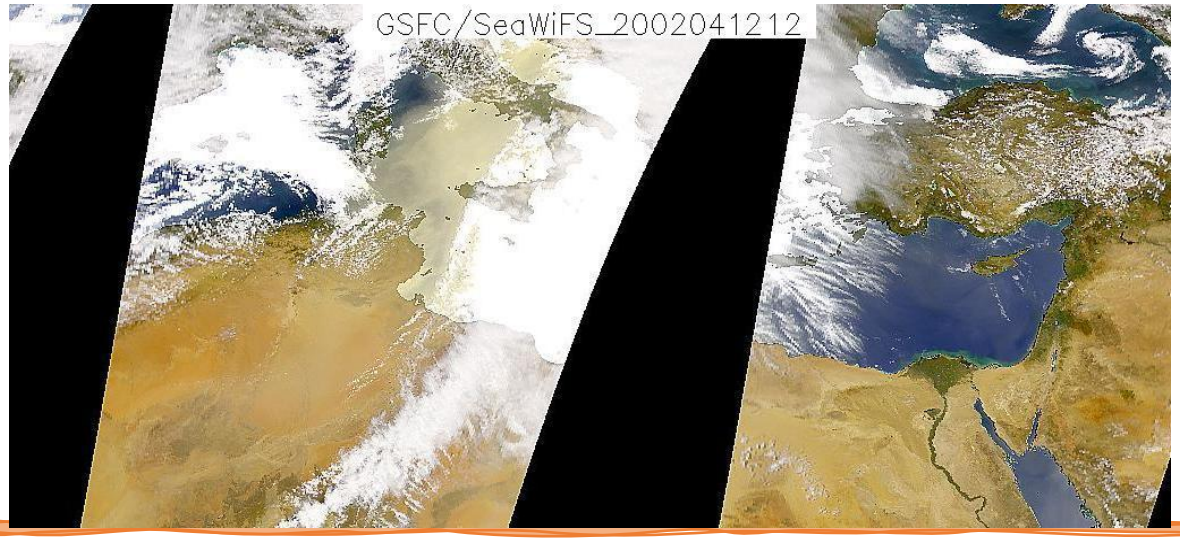

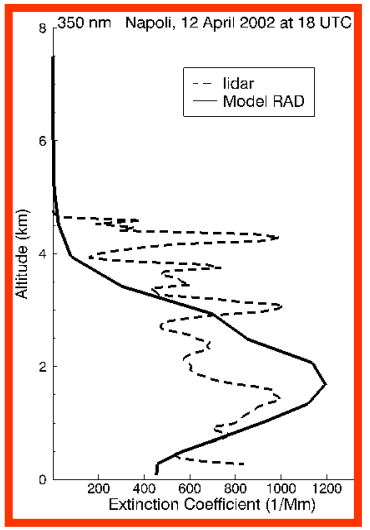

Napoli Raman Lidar

Comparison with observations

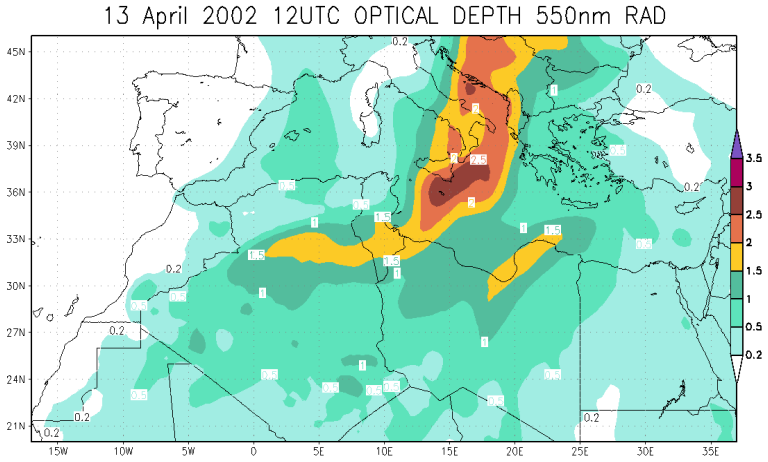

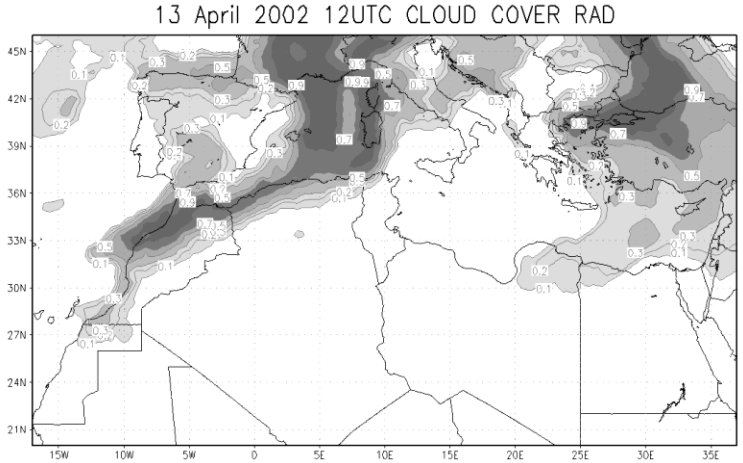

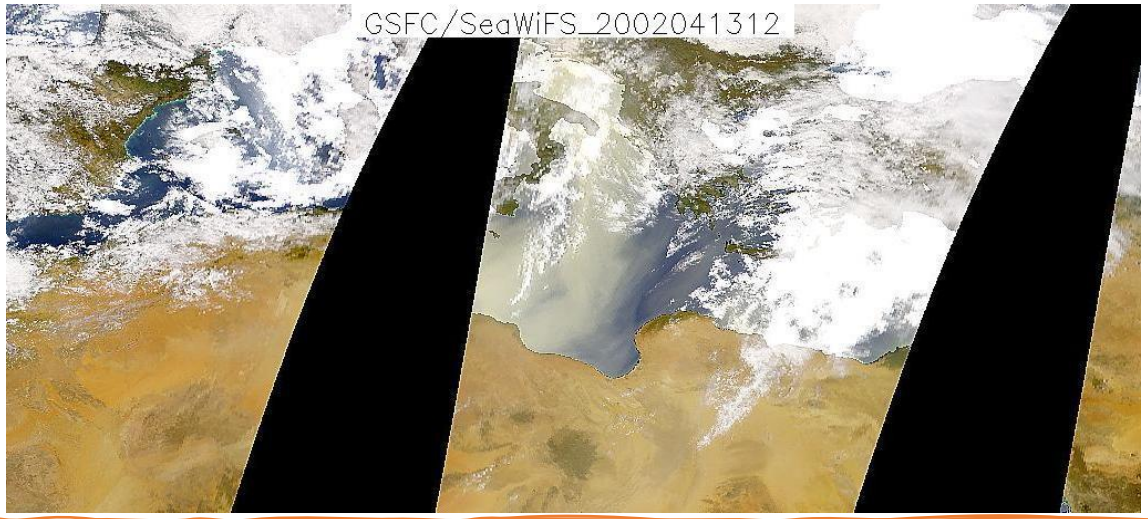

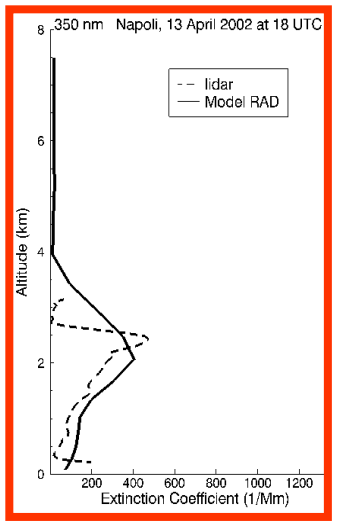

Napoli Raman Lidar

Instantaneous DRE

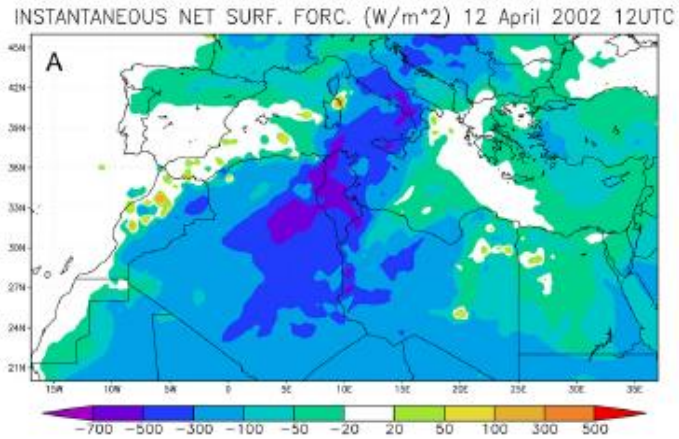

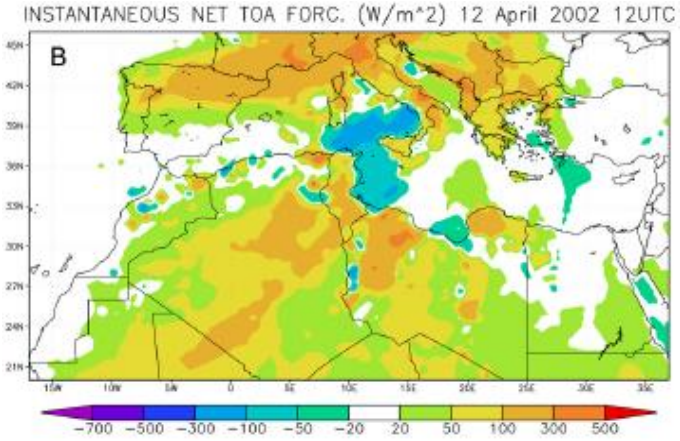

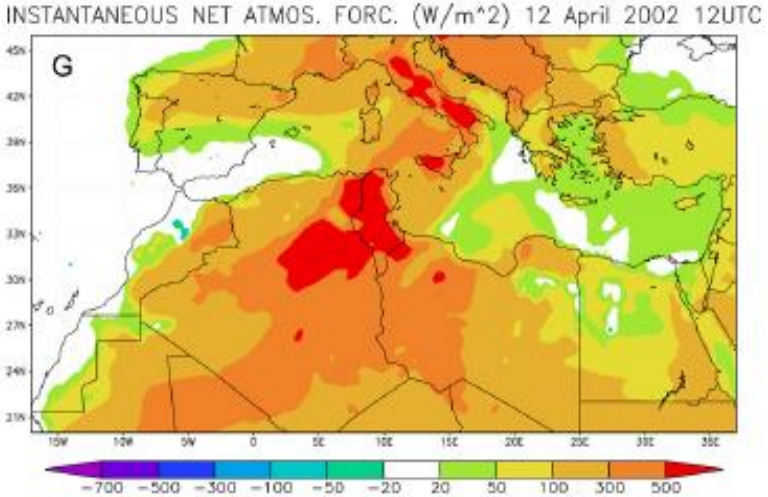

Negative feedbacl upon dust emission

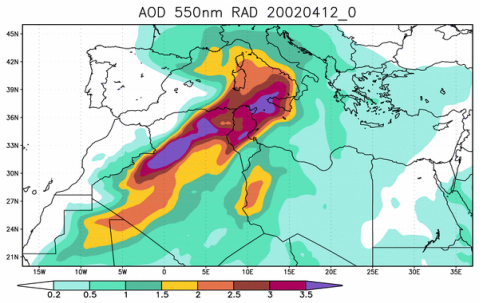

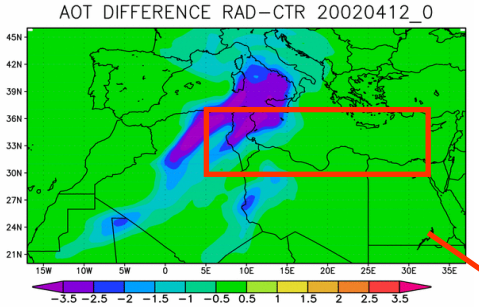

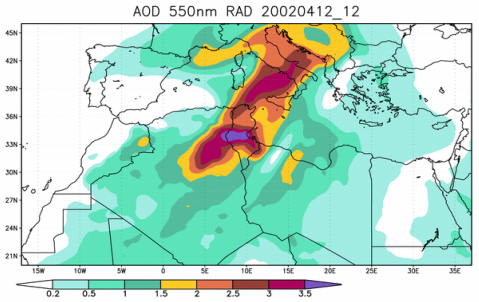

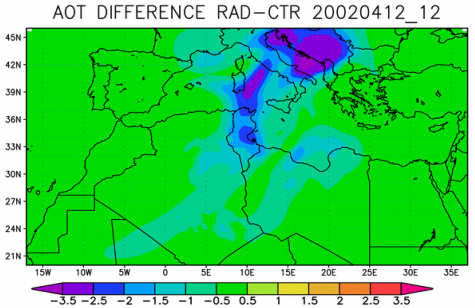

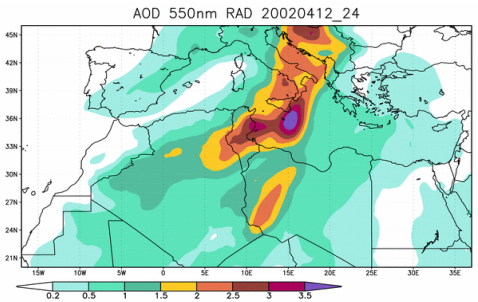

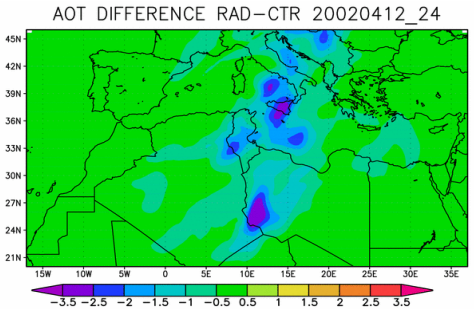

- High spatial correlation between CTR and RAD: 0.95
- 35-45 % reduction of the average AOD over the area covered by the main dust plume

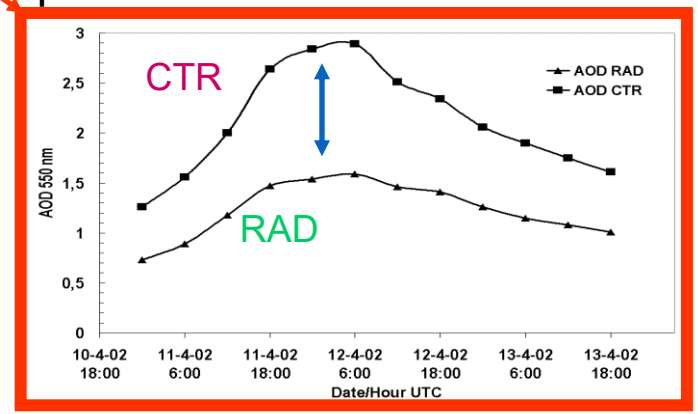

- Strong average negative feedback upon dust emission by dust radiative forcing

Negative feedback upon dust emission

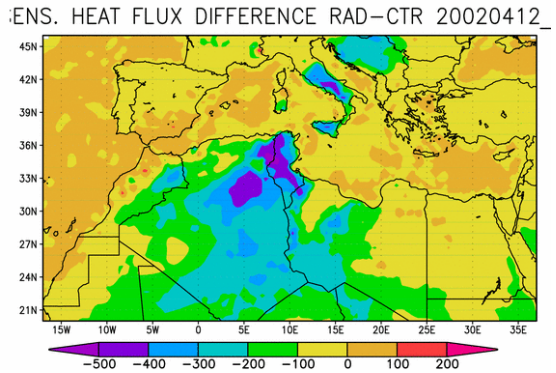

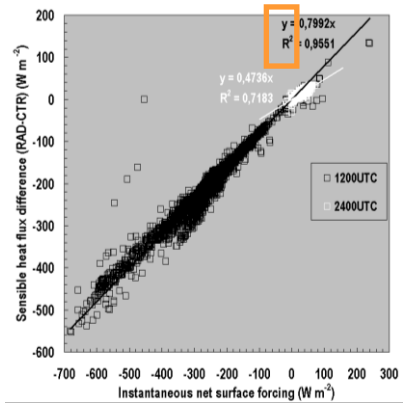

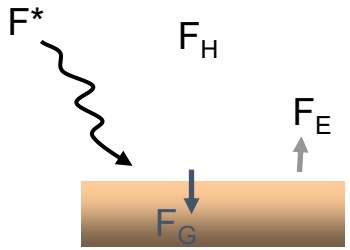

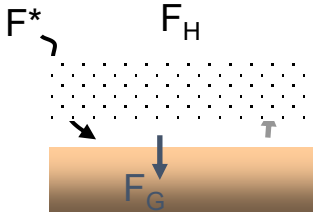

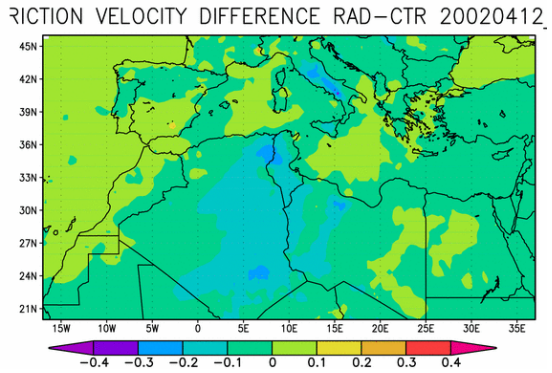

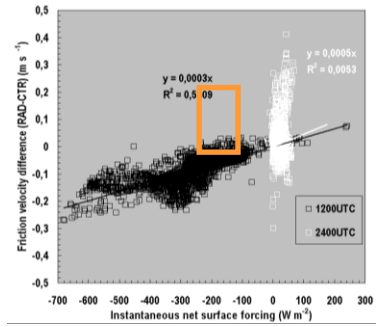

- Negative surface forcing mainly balanced by reduction in turbulent sensible heat flux into the atmosphere

-In RAD mixing is reduced (more stability) and downward momentum is reduced

- Friction velocity significantly correlates with surface forcing during the day

Effects on temperature

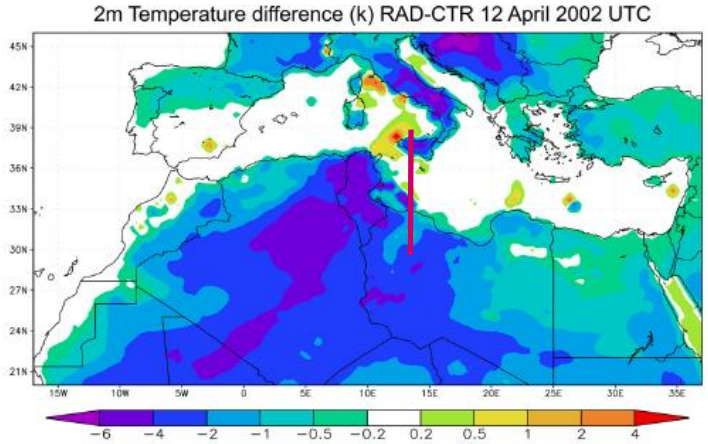

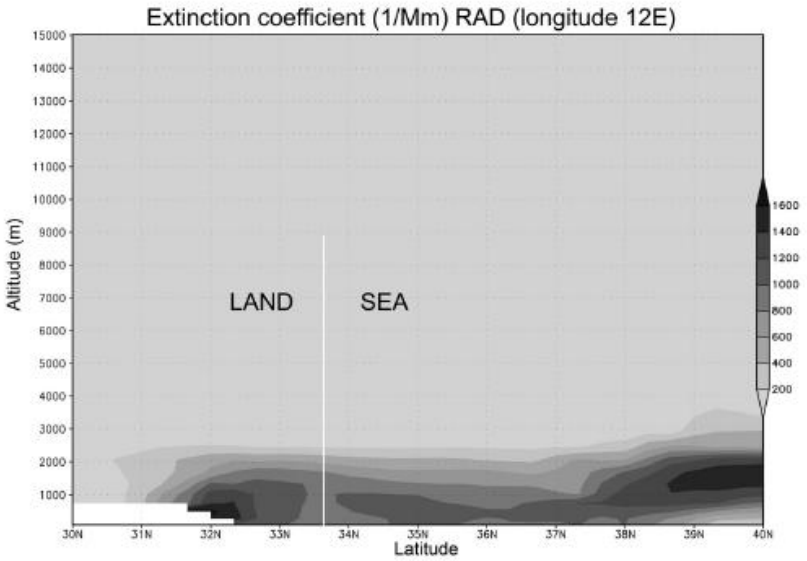

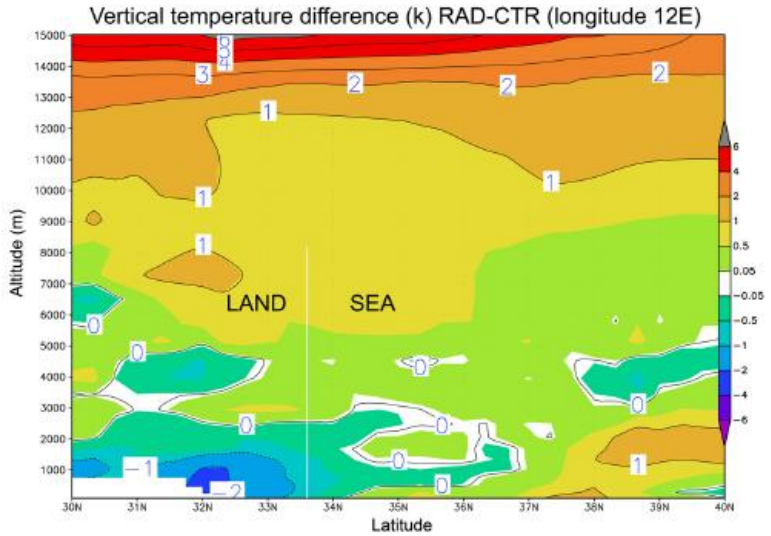

Improvements in temperature forecasts

Atmospheric temperature forecasts
RAD and CTR evaluated against objective analysis data

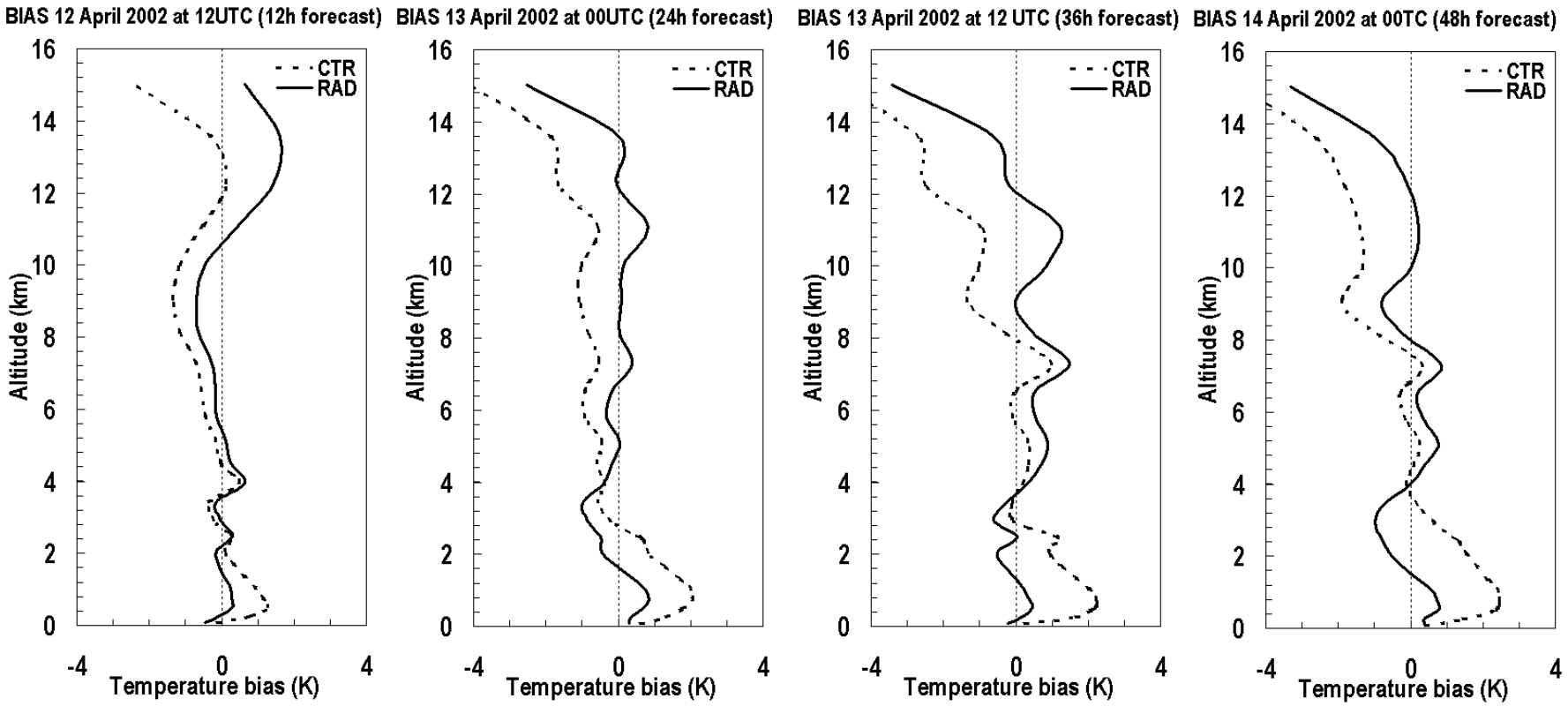

12 h Forecast | 24 h Forecast | 36 h Forecast | 48 h Forecast

Improvements in temperature forecasts

- ✓ RAD improves in most of the atmospheric layers
- ✓ Reduction of the low level warm bias
- ✓ Reduction of the upper level cold bias

WHY?

- ✓ Reduction of sensible heat flux reduces PBL temperature
- ✓ Dust redistributes heat from the surface and near surface to higher levels of the atmosphere

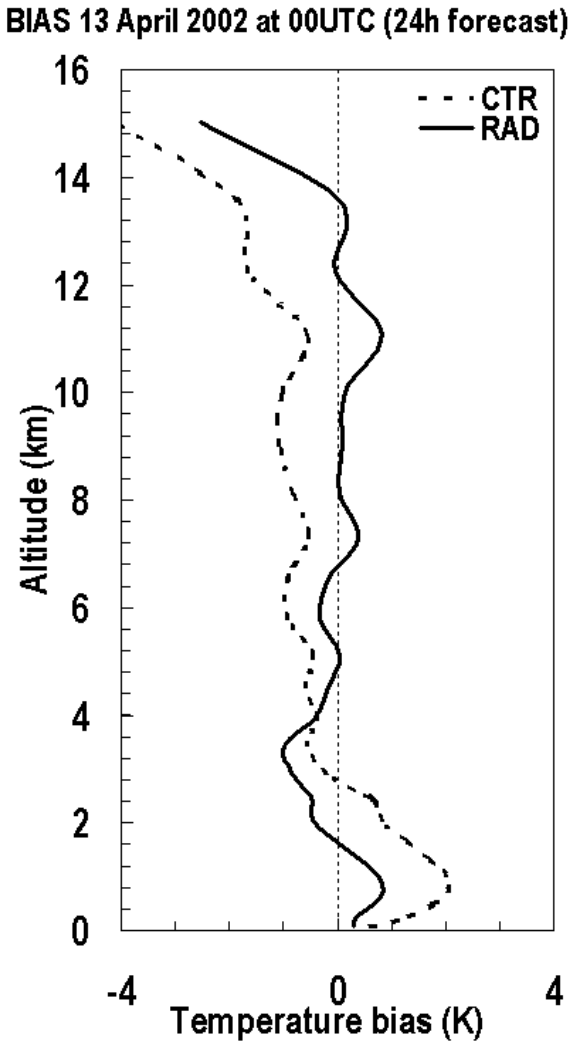

Improvement in SLP forecasts

Sea-level pressure forecasts

- ✓ Positive differences over land
  WHY?
  Colder atmosphere over land suppresses convection and increases subsidence
- ✓ Negative differences over sea
  WHY?
  Dynamical compensation in the direction of the flow

00UTC +24h

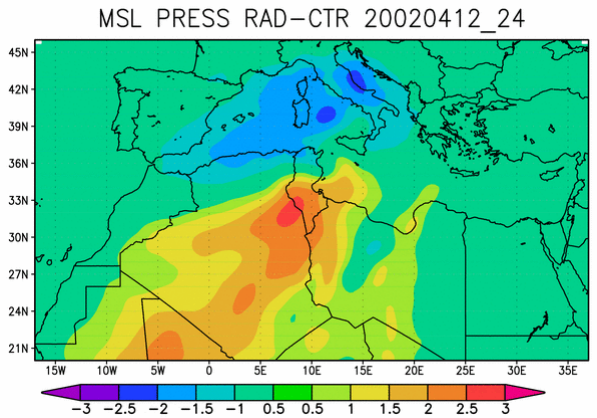

00UTC + 48h

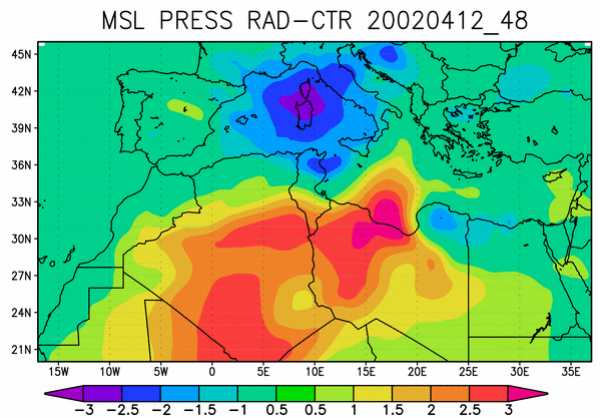

RAD and CTR evaluated against objective analysis data

- ✓ RAD significantly improves the forecast

Root mean square error

	Forecast time			
	12 h	**24 h**	**36 h**	**48 h**
RAD	1.93	1.52	2.29	1.76
CTR	1.95	1.83	2.73	2.09

Funded by the European Union

THANK YOU

This project has received funding from the European Union's Horizon Europe Framework Programme under the grant agreement No 101160258. Views and opinions expressed are however those of the author(s) only and do not necessarily reflect those of the European Union.

ERATOSTHENES CENTRE OF EXCELLENCE · BSC Barcelona Supercomputing Center Centro Nacional de Supercomputación · GRASP · ARMINES · MINES PARIS | PSL · Ciências ULisboa · FCiências.ID · pmod wrc

References

Adebiyi & Kok (2020), Science Advances, https://doi.org/10.1126/sciadv.aaz9507
Adebiyi et al. (2020), Atmospheric Chemistry and Physics, https://doi.org/10.5194/acp-20-829-2020
Claquin et al. (1999), Journal of Geophysical Research: Atmospheres, https://doi.org/10.1029/1999JD900416
Di Biagio et al. (2019), Atmospheric Chemistry and Physics, https://doi.org/10.5194/acp-19-15503-2019
Dubovik et al. (2002), Journal of the Atmospheric Sciences, https://doi.org/10.1175/1520-0469(2002)059%3C0590:VOAAOP%3E2.0.CO;2
Dubovik et al. (2006), Journal of Geophysical Research: Atmospheres, https://doi.org/10.1029/2005JD006619
Gonçalves et al. (2023), Atmospheric Chemistry and Physics, https://doi.org/10.5194/acp-23-8623-2023
Green et al. (2023), IEEE, https://doi.org/10.1109/AERO55745.2023.10115851
Huang et al. (2014), Journal of Geophysical Research: Atmospheres, https://doi.org/10.1002/2014JD021796
Huang et al. (2020), Geophysical Research Letters, https://doi.org/10.1029/2019GL086592
Journet et al. (2014), Atmospheric Chemistry and Physics, https://doi.org/10.5194/acp-14-3801-2014
Kalashnikova & Sokolik (2004), Journal of Quantitative Spectroscopy and Radiative Transfer, https://doi.org/10.1016/j.jqsrt.2003.12.026
Kandler et al. (2009), Tellus B, https://doi.org/10.1111/j.1600-0889.2008.00385.x
Meng et al. (2010), Journal of Aerosol Science, https://doi.org/10.1016/j.jaerosci.2010.02.008
Obiso et al. (2024), Atmospheric Chemistry and Physics, https://doi.org/10.5194/acp-24-5337-2024
Obiso et al. (in rev.), Journal of Geophysical Research: Atmospheres
Pérez et al. (2011), Atmospheric Chemistry and Physics, https://doi.org/10.5194/acp-11-13001-2011
Saito et al. (2021), Journal of the Atmospheric Sciences, https://doi.org/10.1175/JAS-D-20-0338.1
Scanza et al. (2015), Atmospheric Chemistry and Physics, https://doi.org/10.5194/acp-15-537-2015
Schuster et al. (2016), Atmospheric Chemistry and Physics, https://doi.org/10.5194/acp-16-1565-2016
Sinyuk et al. (2020), Atmospheric Measurement Techniques, https://doi.org/10.5194/amt-13-3375-2020
Zhang et al. (2015), Atmospheric Chemistry and Physics, https://doi.org/10.5194/acp-15-12159-2015